The divergent Filamin FLN-2 maintains nuclear integrity during P-cell nuclear migration through constrictions in *Caenorhabditis elegans*

By

LINDA MA

Dissertation

Submitted in partial satisfaction of the requirements for the degree of

Doctor of Philosophy

in

Biochemistry, Molecular, Cellular and Developmental Biology

in the

OFFICE OF GRADUATE STUDIES

of the

UNIVERSITY OF CALIFORNIA

DAVIS

Approved:

Daniel A. Starr, Chair

Lesilee S. Rose

Richard J. McKenney

Committee in Charge

2022

I dedicate this dissertation and the completion of my PhD to those who paved the way. As a first-generation college student, this degree is for my great-grandparents and grandparents (Ma Tien, Cao Lang, Minh Lac, and Quang Bay) whom did not have access to a formal education, my parents (Amy Minh and Tom Ma) who never completed middle school (but always encouraged my intellectual curiosity), and my brother (John Ma) who served as a role model for me to pursue higher education.

Abstract

Cellular migration is essential for an assortment of developmental processes ranging from embryogenesis to neurodevelopment. Oftentimes, cellular migration through narrow spaces is limited by nuclear migration,such as is the case for cancer metastasis and in immune response (i.e. white blood cells rushing to the site of injury). Nuclear migration through small constrictions has been studied *in vitro* but not *in vivo*. Here, we look at nuclear migration in the context of the developing vulval and neural precursors of *Caenorhabditis elegans*. During the mid-L1 larval stage, six pairs of P-cell nuclei migrate from the lateral half of the worm to the ventral cord, where they will divide and progress into the vulval and neural precursor cells. These nuclei must migrate through a constriction between the cuticle and the muscle of the developing animal that is about 5% of the diameter of nucleus in the early L1 stage. We explore the mechanisms which allow them to stably migrate in this normal developmental process. Typically, this process has been facilitated by the microtubule-based SUN-KASH pathway, which serve as the tracks for the migrating nuclei.

Previous studies have shown that in the absence of the SUN-KASH pathway, these nuclei still migrate at 15°C. We found that there is an actin-based pathway which aids the migration process at 15°C in parallel and in absence of the SUN-KASH pathway. We hypothesized that FLN-2, a filamin, crosslinks branched actin networks and organized actin bundles to support stable nuclear migration through narrow spaces. We found that in the absence of *unc-84* (a SUN protein) and/or *fln-2*, that nuclear rupture events were more prevalent in the migrating P cells, while the absence of *unc-84* resulted in the formation of micronuclei in the early and mid-migration stages. We propose future work to determine how FLN-2 may be facilitating P-cell nuclear migration, along with its relationship to UNC-84, LMN-1 (lamin), and CGEF-1 (Cdc42 guanine exchange factor).

Contents

Acknowledgments

I thank my advisor, Dan Starr for his unending support and guidance these past few years in my lab work and career development. Thank you for encouraging and cheering me on while I fought my impostor syndrome and had experimental pitfalls. Your heart is always in the right place, even if your pep talks never landed. Thank you for your patience and feedback on the many iterations of every talk, poster, and paper I have worked on. I was lucky to have you as my PhD mentor and could not have completed this journey without you and your continuing optimism.

Thank you to my dissertation committee members, Lesilee Rose and Rick McKenney, for their unwavering interest in my work and helpful advice and for helping keep me focused and on track.

Thank you to Denneal Jamison-McClung, director of the Designated Emphasis in Biotechnology for taking a vested interest in my career development.

I thank past and present members of my lab and the larger BESt lab for their insights and friendship, especially Hongyan Hao, Jamie Ho, and Ellen Gregory.

I thank my family for their support, and for always believing in me whenever I doubted myself. For being there for me through the good and bad. To my late cat, Milo for keeping me company during the pandemic and my cat, Pippi for being there to keep me company and forcing me to take breaks while I wrote this dissertation.

I thank my friends for their continued encouragement and for helping me live life outside of my academic bubble. Thank you to my friend and cohortmate Jessica Huang for your constant friendship, helping me celebrate the small things, trading baked goods, and being there to help me navigate the bad.

Additional thank you to Bo Liu and Yuh-Ru Julie Lee for their continued interest in my graduate school success. Thank you to participants of Friday Cytoskeleton Club for their helpful questions and comments over the past few years.

Thank you to my mentors at UCLA (Marcus Roper and Tama Hasson) for taking a chance on me and helping me to get to graduate school, for believing in me.

Chapter I: Introduction - The cytoskeleton is tightly integrated with *C. elegans* developmental processes

1.1 Actin is involved in *C. elegans* development

I have spent most of my graduate career trying to characterize the role of actin, actin-binding proteins, and other actin-related players in nuclear migration. Actin is a protein that exists in two forms: monomeric globular (G-actin) and filamentous actin (F-actin) (Dominguez and Holmes, 2011). Our studies focus on the role of F-actin, so I will not expand on G-actin, though the dynamic actin cytoskeleton is integral to many *Caenorhabditis elegans* (*C. elegans*).developmental processes. Each actin filament has a barbed end and a pointed end, growing more rapidly at the barbed end than the pointed end (Winder and Ayscough, 2005).

Many actin binding proteins serve to regulate actin dynamics, including Arp2/3, profilin, capping protein, ADF/ cofilin, and filamins (Pollard and Borisy, 2003; Winder and Ayscough, 2005). The Arp2/3 complex, composed of two actin-related proteins and five other subunits, initiates polymerization of new actin filaments (Pollard and Beltzner, 2002). Profilin is a G-actin binding protein, working to stabilize unpolymerized actin (Schlüter et al., 1997). Capping protein, as the name implies, binds to barbed ends to prevent further actin polymerization (Cooper and Schafer, 2000). ADF/ cofilin enhance actin turnover by regulating actin depolymerization and polymerization (Bamburg et al., 1999). Filamins are mechano-sensing actin cross-linkers (Nakamura et al., 2011a).

Generally, outside of *C. elegans*, actin is involved in cancer metastasis, embryonic development, Alzheimer's disease, and immune response (Pollard and Cooper, 2009). Further, actin is generally responsible for cell shape, mechanical properties, and movement. For instance, actin in the lamellipodia of motile cells support cell movement, as actin subunits turnover, cell movement is coupled to the formation of nascent actin filaments in the leading edge through treadmilling (Theriot and Mitchison, 1991). Actin is very tightly integrated into a variety of processes that are essential to proper *C. elegans* development. Actin can be found in

pronuclear migration, ventral enclosure, Q cell migration, vulva development, fertilization, and as our lab demonstrates, nuclear migration through constricted spaces.

1.2 Pronuclear migration and embryogenesis

One essential *C. elegans* developmental process, pronuclear migration, requires support from cytoskeletal filaments, including microtubules and actin. Microtubules serve as the track for nuclear migration, before they are repositioned on F-actin at the cellular cortex. SUN and KASH proteins serve as part of the LINC (linker of the nucleoskeleton to the cytoskeleton) complex to facilitate this migration and repositioning (Xiong et al., 2011; Bone and Starr, 2016). Arp2/3 has been shown to promote the migration of the male pronucleus to meet the female pronucleus following fertilization (Xiong et al., 2011). Further, they compared their Arp2/3 mutants to *unc-84* mutants (Malone et al., 2003) and found similar male pronuclear migration defects, suggesting actin-dependent microtubule growth (Xiong et al., 2011).

Following fertilization and pronuclear migration, the three principal axes (Anterior-Posterior (AP), dorso-ventral (DV), and LR (left-right)) of the *C. elegans* body plan are set up. Consequently, this process of defining the three principal axes is important for promoting asymmetric cell division to produce six founder cells: AB, MS, E, C, D and P (Sulston et al., 1983). In the thirty minutes after fertilization, the PAR complex (PAR-3, PAR-6, and PKC-3) that maintains cell polarity, is distributed evenly throughout the cortex of the embryo (Munro et al., 2004; Guo and Kemphues, 1995; Hung and Kemphues, 1999; Cuenca et al., 2003; Boyd et al., 1996; Etemad-Moghadam et al., 1995). This PAR complex then localizes to the anterior cortex by cortical flow, in turn, these proteins will promote cortical flow and mediate actomyosin dynamics. The cortical actomyosin meshwork asymmetrically contracts to drive anterior cortical flows of PAR proteins and yolk granules to establish PAR polarity (Munro et al., 2004). Thusly, the AP axis is established, with the first cell division into the AB (anterior blastomere) and the P

(posterior blastomere) cells. These P cells are not to be confused with the hypodermal P cells which we use for my studies in the Starr Lab.

1.3 Ventral Enclosure

Another *C. elegans* developmental process which depends on actin regulation is ventral enclosure. Ventral enclosure occurs in the comma stage *C. elegans* embryo, where a thin epithelial sheet spreads from the lateral part of the embryo and meets at the ventral midline to enclose the worm (**Fig 1.1a-c**) (Chisholm and Hardin, 2005; Williams-Masson et al., 1997). Successful completion of ventral enclosure prevents the GEX phenotype where the C. elegans gut is on the exterior of the animal (Soto et al., 2002). This process is heavily dependent on actin and occurs in two steps: 1) two pairs of leading cells protrude at their medial tips and pull the hypodermis to the center of the embryo, ventral enclosure halts if actin is inhibited during this step (**Fig 1.1a**). 2) an actin ring will form and actomyosin contraction occurs in a 'purse string' mechanism to pull the edges of the hypodermal sheet at the ventral midline (**Fig 1.1b**). Once completed, the hypodermal sheet meets at the ventral midline (**Fig 1.1c**) (Chisholm and Hardin, 2005; Williams-Masson et al., 1997).

During the first step of ventral enclosure, the Soto lab has observed plasma membrane signals (HUM-7, a GTPase-activating protein (GAP) for the RHO-1/RhoA and CDC-42 GTPases) regulating Rac GTPase (upstream of WAVE and Arp2/3) promote branched actin formation (Wallace et al., 2018).

1.4 Q cell migration is regulated by the dynamic actin cytoskeleton

Remodeling of the actin cytoskeletal network plays an important role in initial Q cell migration. Q neuroblasts migrate along the anteroposterior body axis during the L1 larva stage to differentiate into sensory neurons and interneurons (Sulston and Horvitz, 1977; Hedgecock et al., 1987). These neuroblasts undergo three rounds of asymmetric and symmetric divisions,

accompanied by continuous cell migrations. Q neuroblasts can be divided into the QR (right) and QL (left), though identical, these two groups divide at different speeds.

Members of the Rho/Rac-like family of small GTPases: *ced-10*/Rac-1, *rac-2*/Rac1, and *mig-2/*RhoG regulates this dynamic actin network (Lundquist et al., 2001; Zipkin et al., 1997). *ced-10* and *mig-2* allow the Q cells to send out membrane protrusions to facilitate their initial migration (Dyer et al., 2010).

UNC-73/TRIO, a GEF for MIG-2 and CED-10 is also present at the initiation of neuroblast migration. However, UNC-73 mutants express a less severe phenotype than *ced-10; mig-2* double mutants. *mig-2;ced-10* double mutants did not have filopodia-like protrusions, while UNC-73 mutants had similar length, but thinner and highly branched filopodia than wildtype, so there may be other GEFs acting in a redundant role (Kubiseski et al., 2003; Wu et al., 2002). It was shown that *pix-1* acts in parallel to *unc-73* and enhances the *mig-2* mutant phenotype, but not the *ced-10* migration defect (Dyer et al., 2010; Shakir et al., 2006). Interesting enough, these actin remodelers do not affect the direction of Q cell migration.

Q descendant migration is also supported by the dynamic actin network, specifically, *ced-10*/Rac-1, *mig-2*/RhoG, and *ina-1* (integrin α subunit) (Zipkin et al., 1997; Ou and Vale, 2009). *mig-2* and *ina-1* regulate the migration distance and speed of these descendant cells, with mutants migrating at lower speeds and shorter distances. The Vale group believed that these discrepancies between wild-type and *mig-2* mutants were due to lack of persistent polarization (Ou and Vale, 2009). ced-*10; mig-2* with and without *rac-2* RNAi all exhibited more severe migration distance and speed mutations than the single mutants alone (Lundquist et al., 2001; Shakir et al., 2006). The Ou group (Tian et al., 2015) found that MIG-2 recruits Anillin to the leading edge, stabilizing F-actin to allow for cohesive motility. Anillin is an evolutionarily conserved scaffold protein that interacts with actomyosin, septin, microtubules, and the plasma membrane (Oegema et al., 2000; Hickson and O'Farrell, 2008; Field et al., 2005). Anillin is

asymmetrically located at the leading edge during Q cell migration and neurite outgrowth (Tian et al., 2015).

The transmembrane protein, MIG-13, is proposed to transduce an anterior guidance signal to promote QR cell migration in a dosage-dependent manner (Sym et al., 1999). Zhu et al. 2016 (Zhu et al., 2016) identified two semi-redundant Arp2/3 activating pathways: MIG-13-ABL-1-WAVE and MIG-13-SEM-5-WASP. They found that MIG-13 recruits either ABL-1 (an Abl Tyrosine Kinase) or SEM-5 (an adaptor protein) to the leading edge of the cell. Abl-1 recruits WAVE, while SEM-5 recruits WASP, and the MIG-13-ABL-1-WAVE pathway was identified as the main force promoting Q neuroblast motility. The WAVE and WASP pathways then activate the Arp2/3 complex, allowing for actin assembly and subsequent QR migration (Zhu et al., 2016).

unc-34 encodes the *C. elegans* ortholog of Enabled/ VASP, which competes with actin caps, also acts during Q neuroblast migration (Yu et al., 2002; Withee et al., 2004; Shakir et al., 2006). UNC-34 mutants exhibit premature termination of Q cell migration (Shakir et al., 2006). Another very important actin regulator is *cor-1*/ Coronin. Coronin are a conserved family of actin-binding proteins, and the Ou group showed that *cor-1* promotes Q cell migration through actin recycling (Cheng et al., 2013).

1.5 Vulval Development

C. elegans vulval development can be separated into five major steps: 1) generation of VPCs (vulval precursor cells), 2) vulval precursor patterning, 3) generation of adult cells, 4) anchor cell invasion, 5) vulval morphogenesis. Of these five major steps, actin is involved in generation of VCPs, anchor cell invasion, and vulval morphogenesis.

The first step occurs in the larval L1 and L2 stages, where twelve P cells (vulval precursors) are situated along the lateral side of L1 animals. The cells will migrate through a

constricted space between the cuticle and muscle (Bone et al., 2016) (**Fig 1.2B, B'**). If P-cell nuclear migration fails, these worms develop egg-laying deficient (Egl) and uncoordinated (Unc) phenotypes as adults.

There are potentially two or more pathways facilitating P-cell nuclear migration. The first is microtubule-based, and the second is actin-based. The microtubule-based P-cell nuclear migration pathway is facilitated by SUN (UNC-84) and KASH (UNC-83) proteins (Starr et al., 2001; Malone et al., 1999). Sulston and Horvitz found that *unc-84* and *unc-83* null mutants resulted in a temperature-sensitive nuclear migration defect (Sulston and Horvitz, 1981). Our lab conducted a forward genetic screen and found that there were putative actin-adjacent enhancers of the nuclear migration defect of *unc-84* (emu). These were CGEF-1 (CDC-42 GEF) and FLN-2 (a divergent filamin). In these *unc-84* double mutants, the animals recapitulated the Egl and Unc phenotypes at the permissive temperature (15°C) (Chang et al., 2013). It is not yet known how these putative actin players support P-cell nuclear migration. In *unc-84* mutant worms, failed nuclear migration leads to death of the P cell. However, this is not the case for all failed P-cell migration events. In the case of *unc-73* (which encodes a GEF and activates *rho-1*) mutants, P cells fail to fully migrate from the lateral to ventral position. These *unc-73* null animals develop a nonfunctional vulva which is not connected to the uterus and thus the animals are Egl (Spencer et al., 2001).

In step 4, the anchor cell (AC), a specialized uterine cell, breaks down the basement membrane (BM) and forms the vulval-uterine connection in L3 worms (Sherwood and Sternberg, 2003). Dynamic F-actin (invadopodia) are located along the AC's invasive cell membrane to breach the BM (Hagedorn et al., 2013). A yet to be identified vulval precursor signal activates CDC-42 in the AC, leading to activation of the WASP, Arp2/3, WAVE (to a lesser degree), and actin polymerization (Cáceres et al., 2018; Shakir et al., 2008; Lohmer et al., 2016). The Sherwood and Plastino groups found that the AC exerts a high magnitude of

force on the basement membrane, aided by the aforementioned actin players (Cáceres et al., 2018). There is rapid invadopodia turnover, a median life time of 45 secs (Hagedorn et al., 2013). This turnover is regulated by the actin filament severing protein ADF/ cofilin (UNC-60) (Hagedorn et al., 2014). The invadopodia is also reinforced by CED-10 and MIG-2, Rac subfamily Rho GTPases (Hagedorn et al., 2014; Reiner and Lundquist, 2018).

During step 5, these vulval cells then invaginate in the L4 animal and evert in the molt preceding the young adult stage. Vulval morphogenesis, unsurprisingly, requires cytoskeletal reorganization. In addition to being a RHO-1 GEF, UNC-73 serves as a GEF for both CED-10 (a Rac gene involved in distal tip cell migration) and MIG-2 (a divergent Rac gene involved in neuronal cell migration) to orient cell division and migration during vulval morphogenesis (Kishore and Sundaram, 2002).

1.6 The *C. elegans* spermatheca

Actin plays an important regulatory role in the spermatheca. The *C. elegans* spermatheca is where fertilization occurs in the hermaphrodite and is a bag-like structure encapsulated by a myoepithelial layer of sheath cells (Strome, 1986). In the average *C. elegans* hermaphrodite lifetime, each spermatheca goes through ~150 rounds of tightly regulated stretch and contraction to ensure proper entry, fertilization, and exit of the oocyte (Hirsh et al., 1976). The Cram group (Wirshing and Cram, 2017) found that there are stress-fiber like actomyosin bundles along the long axis of each spermathecal cell. These bundles develop with each spermathecal contraction; bundle formation and spermathecal contraction are primarily driven by myosin (Kelley et al., 2018). Spermatheca contraction is regulated by two parallel cooperative pathways: 1) a calcium-dependent pathway (Kovacevic et al., 2013; Kariya et al., 2004), and 2) a Rho-regulated pathway (Tan and Zaidel-Bar, 2015; Wissmann et al., 1999).

In regards to the calcium-dependent pathway, the Cram group (Kovacevic et al., 2013) showed that FLN-1/ filamin and PLC-1/ Phospholipase C-ε are needed to facilitate exit through the sp-ut valve (**sp**ermatheca-**ut**erine valve). Before the first ovulation, the spermathecal cells have unorganized actin bundles and entry promotes calcium oscillations, downstream of FLN-1 (a mechanosensitive actin crosslinker) (DeMaso et al., 2011).

Filamins are actin crosslinkers and bundlers (Nakamura et al., 2011b; Flanagan et al., 2001) with calponin-homology actin binding domains (ABD) and immunoglobulin-like (Ig) repeats (DeMaso et al., 2011; Chen et al., 2013; Nakamura et al., 2007). These Ig repeats facilitates formation of filamin dimers, and interactions with transmembrane proteins and receptors (Loo et al., 1998; Onoprishvili et al., 2003), as well as Rho GTPases (Ohta et al., 1999). Dimerization of filamins imbues filamin-crosslinked actin networks with a high resistance to deformation (Bieling et al., 2016; Gardel et al., 2006; Kolahi and Mofrad, 2008).

There are two filamin homologs in *C. elegans*: FLN-1 and FLN-2. DeMaso et al (DeMaso et al., 2011) examined their structures. At the time of writing, WormBase identifies 20 known isoforms of FLN-1 (a-t). The Cram group found that ceFLN-1 was highly implicated in the release of *C. elegans* fertilized oocytes from the spermatheca (Kovacevic and Cram, 2010; Kovacevic et al., 2013). ceFLN-1 served as a stretch-sensitive structural and signaling scaffold. Upon entry of an oocyte into the spermatheca, PLC-1 releases calcium, while ceFLN-1 sets off the course of IP3-dependent calcium oscillations. These calcium signals propagate through the INX-12 gap junction unit, setting off spermathecal contraction, regulated by MEL-11/myosin phosphatase and NMY-1(non-muscle myosin) (Kovacevic et al., 2013). Further, ceFLN-1's presence was necessary for proper actin organization in the spermatheca and uterus. Phalloidin-stained gonads indicated that FLN-1 spermathecal mutants had thick cortical bundles of F-actin localized to cell-cell junctions compared to regularly spaced circumferential actin

bundles in wildtype. Meanwhile, uterine F-actin was disorganized and lacked the wildtype branching filaments (Kovacevic and Cram, 2010).

In the Rho activated pathway, SPV-1 (Spermatheca Physiology Variant), an F-BAR/ RhoGAP protein, inhibits RhoA activity. When the oocyte enters the spermatheca, SPV-1 detaches from the apical spermathecal membrane and allows RhoA activity to increase in the spermatheca. This Rho activity allows the spermatheca to contract and expel the fertilized oocyte from the sp-ut valve. SPV-1's role allows for cyclical actomyosin contractions (Tan and Zaidel-Bar, 2015). Additionally, a Rho kinase (ROCK) phosphorylates the MRLC (myosin regulatory light chain) and can elevate myosin activity through phosphorylation of myosin phosphatase (Kimura et al., 1996).

The Cram group (Kelley et al., 2018) performed an RNAi screen to identify other kinases that may activate myosin in the spermatheca. They found *mlck-1* (myosin light chain kinase), a Ca2+/CaM-dependent MLCK. MLCK was expressed throughout the spermatheca, while ROCK is found mostly in the distal neck and valve cells (Wissmann et al., 1999). MLCK and ROCK cooperate to perform different roles in the spermatheca to regulate contraction. With MLCK acting as the Ca2+-dependent pathway and ROCK acting in the Rho-activated pathway (Kelley et al., 2018).

1.7 Nuclear migration through constricted space *in vivo*

Cellular migration mediates developmental processes ranging from embryogenesis to neurodevelopment. From yeast to mammals, nuclear migration is an essential part of cellular migration. Reorientation of the MTOC (microtubule-organizing center) and nuclear positioning allow for directional migration in NIH 3T3 fibroblast cells. Rearward nuclear movement was associated by retrograde actin flow and regulated by Cdc42, MRCK, myosin, and actin (Gomes et al., 2005).

In *Saccharomyces cerevisiae*, nuclei must migrate to the mother-bud neck before mitosis and spindle orientation can occur (McMillan and Tatchell, 1994). In growing filamentous fungi, such as *Neurospora crassa* and *Aspergillus nidulans*, there is cytoskeletal-supported transport of nuclei. These nuclei must continually divide and migrate through the syncytium to the advancing hyphal tip (Ma et al., 2016; Gladfelter and Berman, 2009; Roper et al., 2013). Female and male pronuclei must meet for a fertilized zygote to form prior to the first zygotic mitosis (Bajer and Molè-Bajer, 1969; Ungricht and Kutay, 2017a; Ma and Starr, 2020; Rahman et al., 2020).

In contrast to the above examples, some nuclear migrations occur through constricted spaces. In these cases, the nuclei undergo an added level of mechanical stress (Hoffman et al., 2020; Ungricht and Kutay, 2017b). Typically, migration through narrow spaces is limited by nuclear deformability, and the underlying mechanisms participate in hematopoiesis (Shin et al., 2013), immune response (i.e. white blood cells rushing to the site of injury) (Salvermoser et al., 2018), as well as metastatic processes (Seyfried and Huysentruyt, 2013). In hematopoiesis, hematopoietic stem and progenitor cells can be found in adult marrow. When they enter circulation, they must squeeze through the basement membrane and endothelium that separates the blood stream and bone marrow, and is dependent on the level of lamins (Sabin, 1928; Shin et al., 2013). Neutrophils migrate to the sight of injury through an amoeboid migration mode, allowing for high velocity and directed by cell polarization (Salvermoser et al., 2018). They squeeze through junctions and crawl between the endothelial layer and pericyte sheet, followed by interstitial migration to the inflamed tissue (Ley et al., 2007).

Unfortunately, metastatic invasion and proliferation is one of the least understood areas of cancer biology (Seyfried and Huysentruyt, 2013). Tumors can exploit matrix metalloproteinases (MMPs) to degrade collagen and gelatin to avoid migrating through the narrow extracellular matrix (ECM) (Radisky and Radisky, 2010), and the ECM can be a rate-

limiting step in malignant tumor formation and progression (cancer metastasis) (Jackson et al., 2016). In the absence of MMPs, tumors must squeeze and migrate through the ECM, limited by the ability of the nucleus to do so. All of these processes are difficult to study *in vivo.*

1.8 Nuclear migration through constricted spaces *in vitro*

There have been both 2D and 3D explorations of *in vitro* nuclear and cellular migration through constricted spaces. In 2D contexts, these migrating cells are crawling over substrates and need adhesion receptors to anchor them to the surface (Smith et al., 2005; Lammermann and Sixt, 2009). In 3D contexts, these cells are migrating through a matrix or collagen gel surrounding the cell is all directions, allowing for adherence to be more relaxed (Lammermann and Sixt, 2009; Brown, 1982; Haston et al., 1982).

In vitro studies show that metastatic cells can deform and migrate through glass constrictions 5% of their original diameter. The Piel lab placed mouse dendritic cells in PDMS fabricated microchannels with constrictions, plasma bonded to a glass bottom dish, and induced migration. They demonstrated actin enrichment and stable neuronal migration, though it was rate limited by nuclear migration. They found that Arp2/3-driven actin polymerization facilitates nuclear deformation when migrating through narrow spaces (Thiam et al., 2016). They further found that ESCRT III can repair the nuclear envelope when it ruptures during migration through these same chambers. They observed this occurrence in mouse dendritic cells, monocyte-derived human dendritic cells, and HeLa cells (Raab et al., 2016). The Lammerding lab also developed a microfluidic device to examine intra-nuclear deformation through constrictions, consisting of PDMS pillars adhered with a chemotactic gradient to promote cellular migration (Davidson et al., 2015). They corroborated findings that cell migration results in physical stress, nuclear blebbing, and subsequently, rupturing of the nucleus, which requires ESCRT III to repair (Denais et al., 2016).

There have also been studies that use Atomic Force Microscopy to explore strain stiffening at the leading edge of human mammary fibroblasts, human HT1080 wild-type fibrosarcoma, and human SCC38 head and neck squamous cell carcinoma, migrating across fibrillar type I collagen (Van Helvert and Friedl, 2016). The Discher lab used a transwell migration assay coated with fibronectin to provide a 3D space for Glioblastoma-derived U251 cells, lung carcinoma-derived A549 cells, and bone marrow cells. They explored whether altering the lamin-A and lamin-B levels of these cells would affect its ability to migrate. They found that there has to be balance between the two lamins types to ensure that a migrating nucleus is neither too stiff nor too soft (Harada et al., 2014). Although these properties have been quantified *in vitro*, it is important to follow nuclear migration *in vivo* to delineate all the players and inform therapeutic studies. These *in vitro* reconstructions of physiologically relevant substrate do not encapsulate all players that would be present *in vivo*, though they do help provide a fundamental understanding of mechanisms at play.

1.9 Nuclear migration through constricted spaces in *C. elegans*

I propose *Caenorhabditis elegans* as an *in vivo* model given its well-characterized genome and established genetic tools. During development of the early L1 *C. elegans* larva, six pairs of P cells must migrate from the lateral to ventral part of worm, where they then divide and form precursors to the vulva and 12 of 19 GABA neurons. To do so, they must migrate through a narrow constriction about 200nm which is around 5% the size of the P-cell nucleus (5μm) (**Fig. 1.2a-b**) (Cox and Hardin, 2004; Francis and Waterston, 1991). As described previously, the narrow constriction is formed following ventral enclosure and prior to P-cell migration (Chisholm and Hardin, 2005). Fibrous organelles, which disassemble prior to migration (Bone et al., 2016), link the cuticle and muscle, create this constricted space. The P cell migrates between the cuticle and the muscle in order to travel from a lateral to a ventral position. (Hresko et al., 1999; Bercher et al., 2001; Hong et al., 2001; Karabinos et al., 2001).

If P-cell nuclear migration fails, the worm fails to develop a vulva and the proper number of GABA neurons, resulting in Egl (**eg**g-**l**aying deficient) and Unc (**unc**oordinated) phenotypes (Sulston and Horvitz, 1981), which prove to be useful when assaying successful P-cell nuclear migration events (McIntire et al., 1997). *C. elegans* are a good candidate for assaying nuclear migration through constricted spaces *in vivo*, as successful and failed nuclear migration events are easily quantified. Previous work in the lab suggests that P-cell nuclei deform during nuclear migration (Bone et al., 2016), however further work was needed to determine the exact nuclear dynamics during migration.

1.10 LINC complexes and nuclear migration

P-cell nuclear migration is typically facilitated by the SUN (Sad1 and UNC-84)-KASH (Klarsicht, ANC-1 and Syne homology) pathway, where SUN proteins (UNC-84) recruit KASH proteins (UNC-83) to the nuclear envelope (forming a LINC complex, linker of the nucleoskeleton to the cytoskeleton) which then recruit microtubule motors (kinesin-1 and dynein) to coordinate nuclear migration (**Fig 1.3**) (Ho et al., 2018; Meyerzon et al., 2009; Fridolfsson and Starr, 2010; Bone et al., 2016). SUN proteins are located on the inner nuclear membrane and their N-termini interact with lamin in the nucleoplasm. The C-terminal trimeric SUN proteins interact with the C-termini of three KASH peptides (KASH proteins are the outer nuclear membrane protein) in the perinuclear space through a short peptide of ~30 residues known as the KASH domain, and the N-terminus of the KASH protein interacts with microtubule motors in the cytoplasm that facilitate nuclear migration along the microtubules (**Fig 1.3**) (Sosa et al., 2012; Starr, 2019).

When either UNC-84 or UNC-83 is knocked out at the restrictive temperature of 25°C, only 50% of P cells successfully migrate. However, if the SUN-KASH pathway is knocked out at the permissive temperature 15°C, 90% of P cells successfully migrate, indicating a temperature dependent effect on P-cell nuclear migration in the *unc-84(null)* and *unc-83(null)* mutants (Starr

et al., 2001; Malone et al., 1999; Sulston and Horvitz, 1981). This suggests an enhancer pathway is acting in parallel with the SUN-KASH-mediated pathway at the permissive temperature of 15°C.

1.11 Other nuclear migration pathways

Our lab performed a forward genetics screen (Chang et al., 2013) (**Fig 1.4**). This screen allows us to find *emus*, *enhancer of the nuclear migration defect of unc-84*. The screen uses *unc-84(n369)* worms which have a GABA neuron marker, *unc-47::gfp*, and an *unc-84(+); odr-1::rfp* extrachromosomal array. This extrachromosomal array with a wild-type copy of *unc-84* serves as a control in each general of animals, worms which have the extrachromosomal array should be wild-type in all plates. However, their broodmates which lack the extrachromosomal array, if they possess an *emu*, should be *egl* and *unc*. We used EMS (ethyl methanesulfonate) to randomly mutagenize the genomes of our P0 worms. We single our P0 worms, allow them to have progeny and single the F1 generation, making sure to select for the *odr-1::rfp* marker. F1 worms which have the *emu* mutation of interest should be heterozygous for the *emu*. We single the F2 generation, where 25% of our population should be homozygous for the *emu* mutation. Finally, we screen the F3 generation for plates where all worms which lack the extrachromosomal array are *Egl* and *Unc*, while their broodmates on the same plate which have the extrachromosomal array are wild type (**Fig 1.3a**). We then quantify the number of missing GABA neurons to determine whether the mutation we isolated is truly an *emu* (**Fig 1.3b**). This screen found CGEF-1 (Ho et al personal communication) and we uncovered FLN-2 through an RNAi candidate screen (by former lab members Yu-Tai Chang and Jon Kuhn).

CGEF-1 is a predicted CDC-42 (cell division cycle 42) guanine exchange factor. CDC-42 is a small GTPase of the Rho family and a major regulator of cellular polarization, controlling and coordinating many signal transduction pathways (Etienne-Manneville, 2004). CDC-42 cycles between GTP-bound active and GDP-bound inactive states (Etienne-Manneville and

Hall, 2002). CGEF-1 localizes to the cell surface of embryonic cells and when overexpressed is able to stimulate the cycling from a GDP to GTP bound state, activating CDC-42 (Chan and Nance, 2013). Once active, one of the many pathways CDC-42 can take, is to bind to and activate WASp (Wiskott-Aldrich syndrome protein). WASp then activates the Arp2/3 (Actin related protein) complex (Kim et al., 2000; Machesky and Insall, 1999), consisting of seven protein subunits that regulates the formation of a new actin filament at the leading edge of cells at a 70° angle (Mullins et al., 1998). This leads to actin polymerization and formation of filopodia, allowing for cell motility (Pollard and Borisy, 2003).

Generally, filamin dimers respond to mechanical forces applied to F-actin networks. Typically filamin dimers interact with refilin to form actin bundles (Gay et al., 2011). Non-refilin bound filamins will act as actin crosslinkers (Stossel et al., 2001; Janmey and McCulloch, 2007; Razinia et al., 2016). In C. elegans, the Cram lab found that FLN-1 was highly expressed in the spermatheca, uterus, and sheath cells (DeMaso et al., 2011; Kovacevic and Cram, 2010). While FLN-2 was found in the hypodermis, pharynx, intestine, anal depressor muscle, and vulva. Interestingly enough, our isoform of interest, FLN-2C lacks the N-terminal actin binding domain (ABD) that canonical filamins have, and the first three of 15 Ig-like repeats of rod 1 (DeMaso et al., 2011). Further, in mammalian filamins Ig24 is the dimerization domain (Pudas et al., 2005), but ceFLN-2 lacks this domain, and there is no known ortholog of refilin in worms (DeMaso et al., 2011).

1.12 Probing the role of Actin in P-cell nuclear migration

It came as no surprise that actin was involved in P-cell nuclear migration, given its pivotal role in a diverse variety of processes throughout the *Caenorhabditis elegans* lifecycle. It can be found from the germline to larval development to maturation, and acts to regulate embryogenesis, ventral enclosure, Q cell migration, vulval development, and spermathecal contraction among other processes. Its mechanistic involvement in early vulval development of

the P cells required more probing. Further, its interaction with other filamins during *C. elegans* development supported our exploration of FLN-2's interaction with actin during nuclear migration.

Previously, the events linking failed P-cell nuclear migration and cell death were not known. I hypothesize that *fln-2* mediates nuclear migration both in the presence and absence of the microtubule-based pathway, though it is not yet known how. In Chapter Two, I try to determine which isoform of FLN-2 is involved in P-cell nuclear migration present evidence of nuclear rupture in the absence of *unc-84*, with enhanced nuclear rupture in the *fln-2 unc-84* double mutant, suggesting a protective effect on the migrating nucleus as it navigates the narrow constriction bridging the lateral and ventral parts of the P cell. I also examine actin during P-cell nuclear migration. In Chapter Three, I conclude what I have accomplished and observed, and propose future experiments for those who may inherit my project or wish to follow up on questions I have left unsolved.

Figures

Figure 1.1 Ventral enclosure

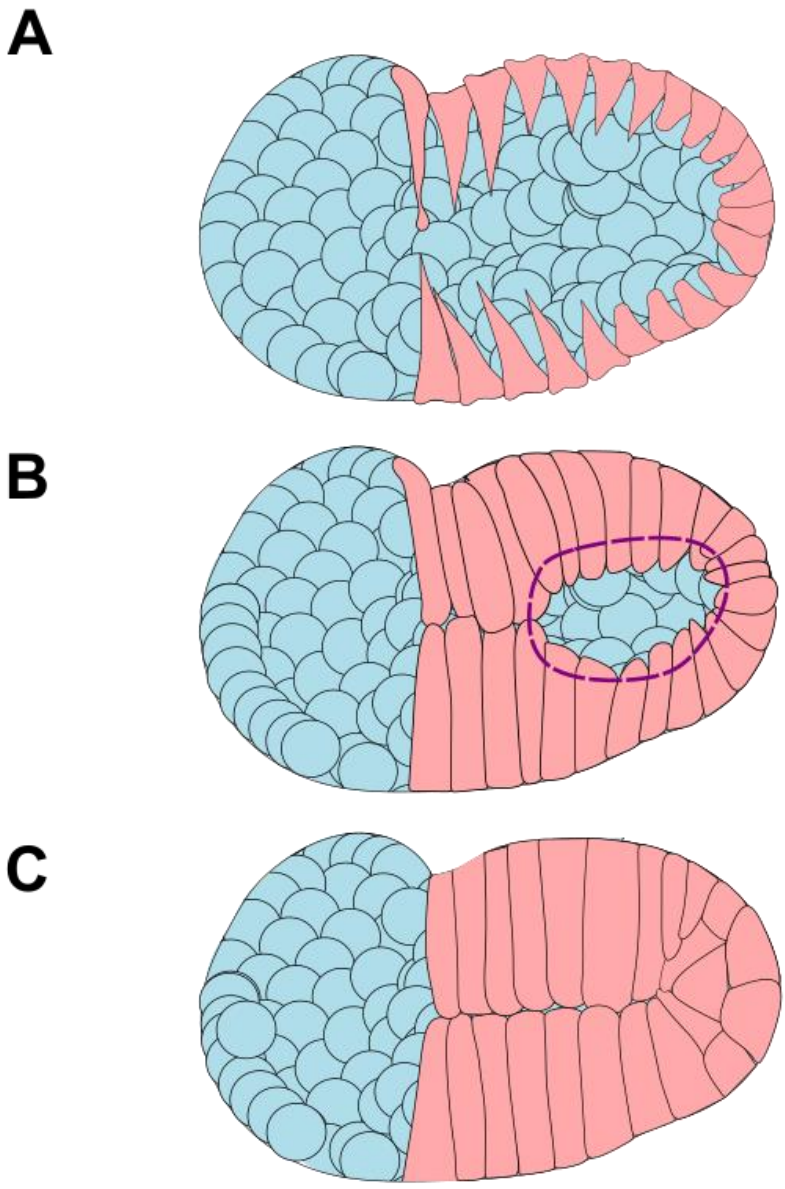

Figure 1.1 Ventral enclosure

This is a depiction of a comma stage *C. elegans* embryo undergoing ventral enclosure. In **A)** The thin epithelial sheet has begun migrating towards the ventral midline. In **B**) the ventral marginal cells are attached to F-actin which form a purse string and contraction of the purse string pulls the hypodermal sheet towards the ventral midline. In **C)** the thin epithelial sheet has migrated to the ventral midline and completed ventral enclosure. The blue cells are neuroblasts

and other internal cells, the pink cells are the thin epithelial sheet originating from the dorsal part of the worm. The purple lines indicate F-actin which has formed a ring.

Figure 1.2 Nuclear migration through constricted spaces in *C. elegans*

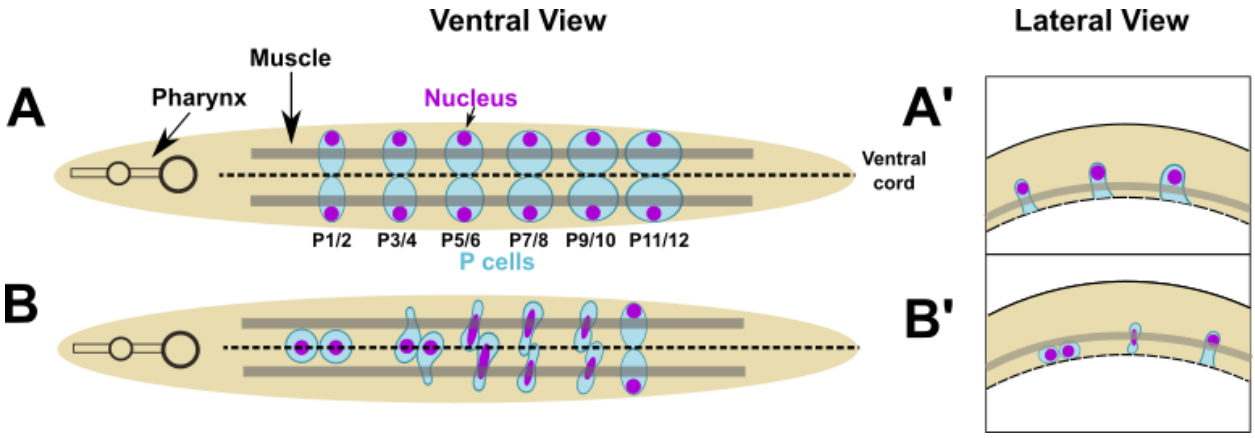

Figure 1.2 Nuclear migration through constricted spaces in *C. elegans*

A, B) A ventral view (**A**) and lateral view (**B**) of P cells during the narrowing and migration stages. P cells are in cyan, nuclei are in magenta, the dashed line indicates the ventral cord. The pharynx indicates the most anterior point of the worm. The muscles are represented by the transparent gray bar overlaying the P cells.

Figure 1.3 The LINC Complex/ SUN-KASH bridge is the canonical pathway that facilitates P-cell nuclear migration

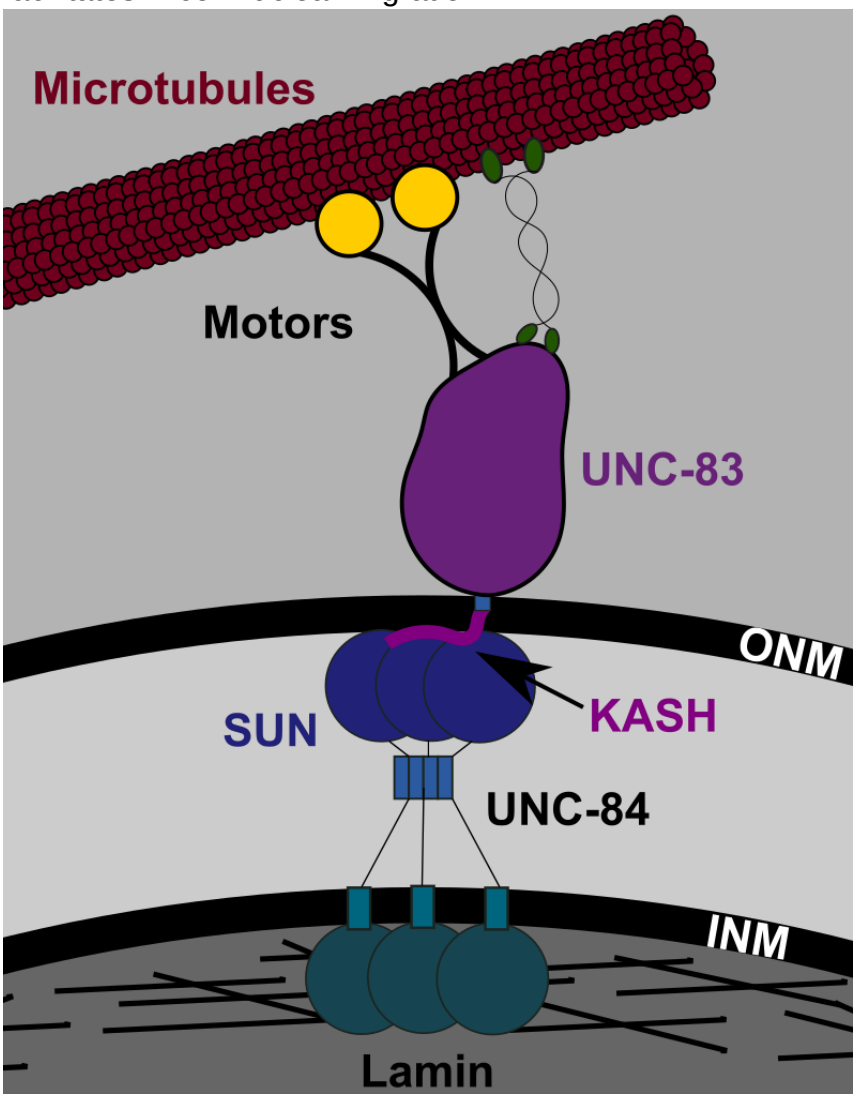

Figure 1.3 The LINC Complex/ SUN-KASH bridge is the canonical pathway that facilitates P-cell nuclear migration

The LINC complex connects the nucleoskeleton to the cytoskeleton. The inner nuclear membrane protein, SUN (UNC-84) interacts with lamin, in the nucleoplasm, and the outer nuclear membrane KASH (UNC-83) in the perinuclear space. UNC-83 interacts with microtubule motors in the cytoplasm, which coordinates nuclear migration along the microtubules. Lamin are the black lines, UNC-84 is shown in dark blue and teal, UNC-83 is shown in purple. The microtubule motors are shown in yellow and green, the microtubules are dark red. The inner and outer nuclear membranes are the black lines and labeled with white text.

Figure 1.4 The enhancer of the nuclear migration of unc-84 screen

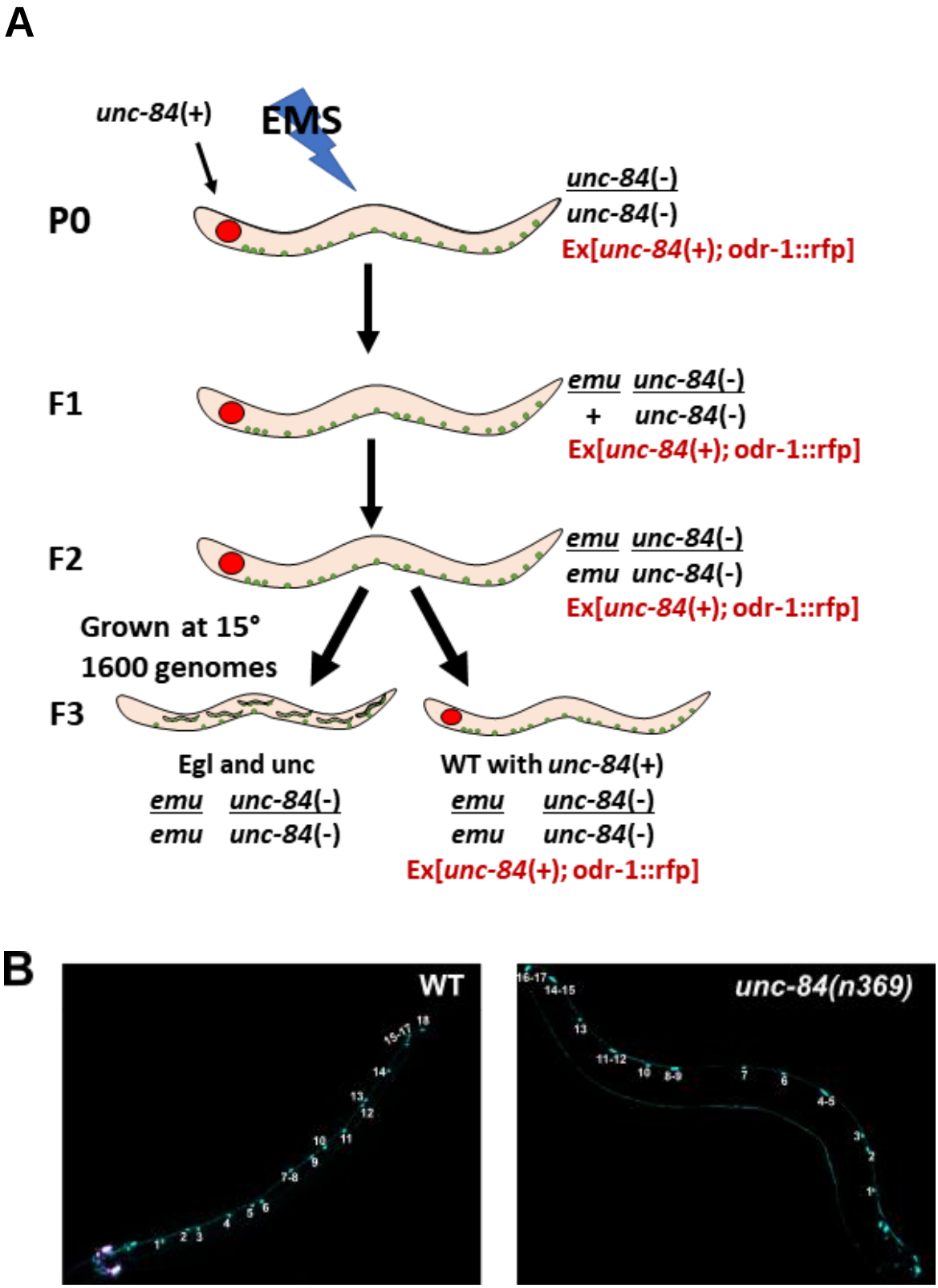

Figure 1.4 The *enhancer of the nuclear migration of unc-84* screen

A) This is the schematic for the entire procedure of the forward enhancer screen we perform to identify *emus* **B)** These are representative images of the GABA neuron secondary assay we perform. The left image depicts *unc-84(n369) +ex[unc-84(n369; odr-1::rfp]* worms which serve as our wild type control, while the right image depicts an *unc-84(n369)* worm.

Citations

Bajer, A., and J. Molè-Bajer. 1969. Formation of spindle fibers, kinetochore orientation, and behavior of the nuclear envelope during mitosis in endosperm - Fine structural and in vitro studies. *Chromosoma*. 27:448–484. doi:10.1007/BF00325682.

Bamburg, J.R., A. McGough, and S. Ono. 1999. Putting a new twist on actin: ADF/cofilins modulate actin dynamics. *Trends Cell Biol.* 9:364–370. doi:10.1016/S0962-8924(99)01619-0.

Bercher, M., J. Wahl, B.E. Vogel, C. Lu, E.M. Hedgecock, D.H. Hall, and J.D. Plenefisch. 2001. mua-3, a gene required for mechanical tissue integrity in Caenorhabditis elegans, encodes a novel transmembrane protein of epithelial attachment complexes. *J. Cell Biol.* 154:415–426. doi:10.1083/jcb.200103035.

Bieling, P., T.-D. De Li, J. Weichsel, R. McGorty, P. Jreij, B. Huang, D.A.A. Fletcher, and R.D.D. Mullins. 2016. Force Feedback Controls Motor Activity and Mechanical Properties of Self-Assembling Branched Actin Networks. *Cell*. 164:115–127. doi:10.1016/j.cell.2015.11.057.

Bone, C., Y.-T. Chang, N.E. Cain, S.P. Murphy, and D.A. Starr. 2016. Nuclei migrate through constricted spaces using microtubule motors and actin networks in C. elegans hypodermal cells. *Development*. 143:4193–4202.

Bone, C.R., and D.A. Starr. 2016. Nuclear migration events throughout development. *J. Cell Sci.* 129:1951–1961. doi:doi:10.1242/jcs.179788.

Boyd, L., S. Quo, D. Levitan, D.T. Stinchcomb, and K.J. Kemphues. 1996. PAR-2 is asymmetrically distributed and promotes association of P granules and PAR-1 with the cortex in C. elegans embryos. *Development*. 122:3075–3084. doi:10.1242/dev.122.10.3075.

Brown, A.F. 1982. Neutrophil granulocytes: Adhesion and locomotion on collagen substrata and in collagen matrices. *J. Cell Sci.* Vol. 58:455–467. doi:10.1242/jcs.58.1.455.

Cáceres, R., N. Bojanala, L.C. Kelley, J. Dreier, J. Manzi, F. Di Federico, Q. Chi, T. Risler, I. Testa, D.R. Sherwood, and J. Plastino. 2018. Forces drive basement membrane invasion in Caenorhabditis elegans. *Proc. Natl. Acad. Sci. U. S. A.* 201808760. doi:10.1073/pnas.1808760115.

Chan, E., and J. Nance. 2013. Mechanisms of CDC-42 activation during contact-induced cell polarization. *J. Cell Sci.* 126:1692–1702. doi:10.1242/jcs.124594.

Chang, Y.-T., D. Dranow, J. Kuhn, M. Meyerzon, M. Ngo, D. Ratner, K. Warltier, and D.A. Starr. 2013. toca-1 Is in a Novel Pathway That Functions in Parallel with a SUN-KASH Nuclear Envelope Bridge to Move Nuclei in Caenorhabditis elegans. *Genetics*. 193:187–200.

Chen, H., S. Chandrasekar, M.P. Sheetz, T.P. Stossel, F. Nakamura, and J. Yan. 2013. Mechanical perturbation of filamin A immunoglobulin repeats 20-21 reveals potential non-equilibrium mechanochemical partner binding function. *Sci. Rep.* 3:1642. doi:10.1038/srep01642.

Cheng, Z., P. Yi, X. Wang, Y. Chai, G. Feng, Y. Yang, X. Liang, Z. Zhu, W. Li, and G. Ou. 2013. Conditional targeted genome editing using somatically expressed TALENs in C. elegans. *Nat. Biotechnol.* 31:934–937. doi:10.1038/nbt.2674.

Chisholm, A.D., and J. Hardin. 2005. Epidermal morphogenesis. *WormBook*. 1–22. doi:10.1895/wormbook.1.35.1.

Cooper, J.A., and D.A. Schafer. 2000. Control of actin assembly and disassembly at filament ends. *Curr. Opin. Cell Biol.* 12:97–103. doi:10.1016/S0955-0674(99)00062-9.

Cox, E.A., and J. Hardin. 2004. Sticky worms: Adhesion complexes in C. elegans. *J. Cell Sci.* 117:1885–1897. doi:10.1242/jcs.01176.

Cuenca, A.A., A. Schetter, D. Aceto, K. Kemphues, and G. Seydoux. 2003. Polarization of the C. elegans zygote proceeds via distinct establishment and maintenance phases. *Development*. 130:1255–1265. doi:10.1242/dev.00284.

Davidson, P.M., J. Sliz, P. Isermann, C. Denais, and J. Lammerding. 2015. Design of a microfluidic device to quantify dynamic intra-nuclear deformation during cell migration through confining environments. *Integr. Biol. (United Kingdom)*. 7:1534–1546. doi:10.1039/c5ib00200a.

DeMaso, C.R., I. Kovacevic, A. Uzun, and E.J. Cram. 2011. Structural and Functional Evaluation of C. elegans Filamins FLN-1 and FLN-2. *PLoS One*. 6:e22428. doi:10.1371/journal.pone.0022428.

Denais, C.., R.M. Gilbert, P. Isermann, A.L. McGregor, M. te Lindert, B. Weigelin, P.M. Davidson, P. Friedl, K. Wolf, and J. Lammerding. 2016. Nuclear envelope rupture and repair during cancer cell migration. *Science (80-.).* 352:353–358.

Dominguez, R., and K.C. Holmes. 2011. Actin Structure and Function. *Annu. Rev. Biophys.* 40:169–186. doi:10.1146/annurev-biophys-042910-155359.

Dyer, J.O., R.S. Demarco, and E.A. Lundquist. 2010. Distinct roles of Rac GTPases and the UNC-73/Trio and PIX-1 Rac GTP exchange factors in neuroblast protrusion and migration in C. elegans. *Small GTPases*. 1:44–61. doi:10.4161/sgtp.1.1.12991.

Etemad-Moghadam, B., S. Guo, and K.J. Kemphues. 1995. Asymetrically Distributed PAR-3 Protein Contributes to Cell Polarity and Spindle Alignment in Early C. elegans Embryos. *Cell*. 83:743–752.

Etienne-Manneville, S. 2004. Cdc42 - the centre of polarity. *J. Cell Sci.* 117:1291–1300. doi:10.1242/jcs.01115.

Etienne-Manneville, S., and A. Hall. 2002. Rho GTPases in cancer cell biology. *Nature*. 420:629–635. doi:10.1016/j.febslet.2008.04.039.

Field, C.M., M. Coughlin, S. Doberstein, T. Marty, and W. Sullivan. 2005. Characterization of anillin mutants reveals essential roles in septin localization and plasma membrane integrity. *Development*. 132:2849–2860. doi:10.1242/dev.01843.

Flanagan, L.A., J. Chou, H. Falet, R. Neujahr, J.H. Hartwig, and T.P. Stossel. 2001. Filamin A, the Arp2/3 complex, and the morphology and function of cortical actin filaments in human melanoma cells. *J. Cell Biol.* 155:511–517. doi:10.1083/jcb.200105148.

Francis, R., and R.H. Waterston. 1991. Muscle cell attachment in Caenorhabditis elegans. *J. Cell Biol.* 114:465–479. doi:10.1083/jcb.114.3.465.

Fridolfsson, H.N., and D.A. Starr. 2010. Kinesin-1 and dynein at the nuclear envelope mediate the bidirectional migrations of nuclei. *J. Cell Biol.* 191.

Gardel, M.L., F. Nakamura, J.H. Hartwig, J.C. Crocker, T.P. Stossel, and D.A. Weitz. 2006. Prestressed F-actin networks cross-linked by hinged filamins replicate mechanical properties of cells. *Proc. Natl. Acad. Sci. U. S. A.* 103:1762–1767. doi:10.1073/pnas.0504777103.

Gay, O., B. Gilquin, F. Nakamura, Z.A. Jenkins, R. McCartney, D. Krakow, A. Deshiere, N. Assard, J.H. Hartwig, S.P. Robertsone, and J. Baudier. 2011. RefilinB (FAM101B) targets FilaminA to organize perinuclear actin networks and regulates nuclear shape. *Proc. Natl. Acad. Sci. U. S. A.* 108:11464–11469. doi:10.1073/pnas.1104211108.

Gladfelter, A., and J. Berman. 2009. Dancing genomes: fungal nuclear positioning. *Nat. Rev. Microbiol.* 7:875–886.

Gomes, E.R., S. Jani, and G.G. Gundersen. 2005. Nuclear Movement Regulated by Cdc42, MRCK, Myosin, and Actin Flow Establishes MTOC Polarization in Migrating Cells. *Cell*. 121:451–463. doi:https://doi.org/10.1016/j.cell.2005.02.022.

Guo, S., and K.J. Kemphues. 1995. par-1, a gene required for establishing polarity in C. elegans embryos, encodes a putative Ser/Thr kinase that is asymmetrically distributed. *Cell*. 81:611–620. doi:10.1016/0092-8674(95)90082-9.

Hagedorn, E.J., L.C. Kelley, K.M. Naegeli, Z. Wang, Q. Chi, and D.R. Sherwood. 2014. ADF/cofilin promotes invadopodial membrane recycling during cell invasion in vivo. *J. Cell Biol.* 204:1209–1218. doi:10.1083/jcb.201312098.

Hagedorn, E.J., J.W. Ziel, M.A. Morrissey, L.M. Linden, Z. Wang, Q. Chi, S.A. Johnson, and D.R. Sherwood. 2013. The netrin receptor DCC focuses invadopodia-driven basement membrane transmigration in vivo. *J. Cell Biol.* 201:903–913. doi:10.1083/jcb.201301091.

Harada, T., J. Swift, J. Irianto, J.W. Shin, K.R. Spinler, A. Athirasala, R. Diegmiller, P.C.D.P. Dingal, I.L. Ivanovska, and D.E. Discher. 2014. Nuclear lamin stiffness is a barrier to 3D migration, but softness can limit survival. *J. Cell Biol.* 204:669–682. doi:10.1083/jcb.201308029.

Haston, W.S., J.M. Shields, and P.C. Wilkinson. 1982. Lymphocyte locomotion and attachment on two-dimensional surfaces and in three-dimensional matrices. *J. Cell Biol.* 92:747–752. doi:10.1083/jcb.92.3.747.

Hedgecock, E.M., J.G. Culotti, D.H. Hall, and B.D. Stern. 1987. Genetics of cell and axon migrations in Caenorhabditis elegans. *Development*. 100:365–382.

Van Helvert, S., and P. Friedl. 2016. Strain Stiffening of Fibrillar Collagen during Individual and Collective Cell Migration Identified by AFM Nanoindentation. *ACS Appl. Mater. Interfaces*. 8:21946–21955. doi:10.1021/acsami.6b01755.

Hickson, G.R.X., and P.H. O'Farrell. 2008. Rho-dependent control of anillin behavior during cytokinesis. *J. Cell Biol.* 180:285–294. doi:10.1083/jcb.200709005.

Hirsh, D., D. Oppenheim, and M. Klass. 1976. Development of the reproductive system of Caenorhabditis elegans. *Dev. Biol.* 49:200–219. doi:10.1016/0012-1606(76)90267-0.

Ho, J., V.A. Valdez, L. Ma, and D.A. Starr. 2018. Characterizing Dynein' s Role in P-cell Nuclear Migration using an Auxin-Induced Degradation System. 1:2016–2018.

Hoffman, L.M., M.A. Smith, C.C. Jensen, M. Yoshigi, and V.M. Weaver. 2020. Mechanical stress triggers nuclear remodeling and the formation of transmembrane actin nuclear lines

with associated nuclear pore complexes. doi:10.1091/mbc.E19-01-0027.

Hong, L., T. Elbl, J. Ward, C. Franzini-Armstrong, K.K. Rybicka, B.K. Gatewood, D.L. Baillie, and E.A. Bucher. 2001. MUP-4 is a novel transmembrane protein with functions in epithelial cell adhesion in Caenorhabditis elegans. *J. Cell Biol.* 154:403–414. doi:10.1083/jcb.200007075.

Hresko, M.C., L.A. Schriefer, P. Shrimankar, and R.H. Waterston. 1999. Adhesion in Caenorhabditis elegans. 146:659–672.

Hung, T.J., and K.J. Kemphues. 1999. PAR-6 is a conserved PDZ domain-containing protein that colocalizes with PAR-3 in Caenorhabditis elegans embryos. *Development*. 126:127–135. doi:10.1242/dev.126.1.127.

Jackson, H.W., V. Defamie, P. Waterhouse, and R. Khokha. 2016. TIMPs: versatile extracellular regulators in cancer. 17:38. doi:10.1038/nrc.2016.115https://www.nature.com/articles/nrc.2016.115#supplementary-information.

Janmey, P.A., and C.A. McCulloch. 2007. Cell mechanics: Integrating cell responses to mechanical stimuli. *Annu. Rev. Biomed. Eng.* 9:1–34. doi:10.1146/annurev.bioeng.9.060906.151927.

Karabinos, A., H. Schmidt, J. Harborth, R. Schnabel, and K. Weber. 2001. Essential roles for four cytoplasmic intermediate filament proteins in Caenorhabditis elegans development. *Proc. Natl. Acad. Sci. U. S. A.* 98:7863–7868. doi:10.1073/pnas.121169998.

Kariya, K.I., Y. Kim Bui, X. Gao, P.W. Sternberg, and T. Kataoka. 2004. Phospholipase Cε regulates ovulation in Caenorhabditis elegans. *Dev. Biol.* 274:201–210. doi:10.1016/j.ydbio.2004.06.024.

Kelley, C.A., A.C.E. Wirshing, R. Zaidel-Bar, and E.J. Cram. 2018. The myosin light-chain kinase MLCK-1 relocalizes during Caenorhabditis elegans ovulation to promote actomyosin bundle assembly and drive contraction. *Mol. Biol. Cell*. 29:1975–1991. doi:10.1091/mbc.E18-01-0056.

Kim, A.S., L.T. Kakalis, N. Abdul-Manan, G.A. Liu, and M.K. Rosen. 2000. Autoinhibition and activation mechanisms of the Wiskott-Aldrich syndrome protein. *Nature*. 404:151–158. doi:10.1038/35004513.

Kimura, K., M. Ito, M. Amano, K. Chihara, Y. Fukata, K. Kimura, M. Ito, and M. Amano. 1996. Regulation of Myosin Phosphatase by Rho and Rho-Associated Kinase (Rho- Kinase) Masato Nakafuku , Bunpei Yamamori , Jianhua Feng , Takeshi Nakano , Katsuya Okawa , Akihiro Iwamatsu and Kozo Kaibuchi Published by : American Association for the Advancemen. *Science (80-.).* 273:245–248.

Kishore, R.S., and M. V Sundaram. 2002. ced-10 Rac and mig-2 Function Redundantly and Act with unc-73 Trio to Control the Orientation of Vulval Cell Divisions and Migrations in Caenorhabditis elegans. 348:339–348. doi:10.1006/dbio.2001.0513.

Kolahi, K.S., and M.R.K. Mofrad. 2008. Molecular Mechanics of Filamin's Rod Domain. *Biophys. J.* 94:1075–1083. doi:10.1529/biophysj.107.118802.

Kovacevic, I., and E.J. Cram. 2010. FLN-1/Filamin is Required for Maintenance of Actin and Exit of Fertilized Oocytes from the Spermatheca in C. elegans. *Dev. Biol.* 347:247–257. doi:10.1016/j.ydbio.2010.08.005.

Kovacevic, I., J.M. Orozco, and E.J. Cram. 2013. Filamin and Phospholipase C- e Are Required for Calcium Signaling in the Caenorhabditis elegans Spermatheca. 9. doi:10.1371/journal.pgen.1003510.

Kubiseski, T.J., J. Culotti, and T. Pawson. 2003. Functional Analysis of the Caenorhabditis elegans UNC-73B PH Domain Demonstrates a Role in Activation of the Rac GTPase In Vitro and Axon Guidance In Vivo. *Mol. Cell. Biol.* 23:6823–6835. doi:10.1128/mcb.23.19.6823-6835.2003.

Lammermann, T., and M. Sixt. 2009. Mechanical modes of ' amoeboid ' cell migration. *Curr. Opin. Cell Biol.* 21:636–644. doi:10.1016/j.ceb.2009.05.003.

Ley, K., C. Laudanna, M.I. Cybulsky, and S. Nourshargh. 2007. Getting to the site of inflammation: The leukocyte adhesion cascade updated. *Nat. Rev. Immunol.* 7:678–689. doi:10.1038/nri2156.

Lohmer, L.L., M.R. Clay, K.M. Naegeli, Q. Chi, J.W. Ziel, E.J. Hagedorn, J.E. Park, R. Jayadev, and D.R. Sherwood. 2016. A Sensitized Screen for Genes Promoting Invadopodia Function In Vivo: CDC-42 and Rab GDI-1 Direct Distinct Aspects of Invadopodia Formation. *PLoS Genet.* 12:1–29. doi:10.1371/journal.pgen.1005786.

Loo, D.T., S.B. Kanner, and A. Aruffo. 1998. Filamin binds to the cytoplasmic domain of the β1-integrin: Identification of amino acids responsible for this interaction. *J. Biol. Chem.* 273:23304–23312. doi:10.1074/jbc.273.36.23304.

Lundquist, E.A., P.W. Reddien, E. Hartwieg, H. Robert Horvitz, and C.I. Bargmann. 2001. Three C. elegans Rac proteins and several alternative Rac regulators control axon guidance, cell migration and apoptotic cell phagocytosis. *Development*. 128:4475–4488.

Ma, L., B. Song, T. Curran, N. Phong, E. Dressaire, and M. Roper. 2016. Defining individual size in the model filamentous fungus Neurospora crassa. *Proc. R. Soc. B Biol. Sci.* 283. doi:10.1098/rspb.2015.2470.

Ma, L., and D.A. Starr. 2020. Membrane fusion drives pronuclear meeting in the one-cell embryo. *J. Cell Biol.* 219. doi:10.1083/jcb.202001048.

Machesky, L.M., and R.H. Insall. 1999. Signaling to actin dynamics. *J. Cell Biol.* 146:267–272. doi:10.1083/jcb.146.2.267.

Malone, C.J., W.D. Fixsen, H.R. Horvitz, and M. Han. 1999. UNC-84 localizes to the nuclear envelope and is required for nuclear migration and anchoring during C. elegans development. *Development*. 126:3171–3181.

Malone, C.J., L. Misner, N. Le Bot, M.-C. Tsai, J.M. Campbell, J. Ahringer, and J.G. White. 2003. The C. elegans Hook Protein, ZYG-12, Mediates the Essential Attachment between the Centrosome and Nucleus. *Cell*. 115:825–836. doi:https://doi.org/10.1016/S0092-8674(03)00985-1.

McIntire, S.L., R.J. Reimer, K. Schuske, R.H. Edwards, and E.M. Jorgensen. 1997. Identification and characterization of the vesicular GABA transporter. *Nature*. 389:870–876. doi:10.1038/39908.

McMillan, J.N., and K. Tatchell. 1994. The JNM1 Gene in the Yeast Saccharomyces cerevisiae Is Required for Nuclear Migration and Spindle Orientation During the Mitotic Cell Cycle. *J. Cell B*. 125:143–158.

Meyerzon, M., H.N. Fridolfsson, N. Ly, F.J. McNally, and D.A. Starr. 2009. UNC-83 is a nuclear-specific cargo adaptor for kinesin-1-mediated nuclear migration. *Development*. 136:2725–2733. doi:10.1242/dev.038596.

Mullins, R.D., J.A. Heuser, and T.D. Pollard. 1998. The interaction of Arp2/3 complex with actin: Nucleation, high affinity pointed end capping, and formation of branching networks of filaments. *Proc. Natl. Acad. Sci. U. S. A.* 95:6181–6186. doi:10.1073/pnas.95.11.6181.

Munro, E., J. Nance, and J.R. Priess. 2004. Cortical flows powered by asymmetrical contraction transport PAR proteins to establish and maintain anterior-posterior polarity in the early C. elegans embryo. *Dev. Cell*. 7:413–424. doi:10.1016/j.devcel.2004.08.001.

Nakamura, F., T.M. Osborn, C.A. Hartemink, J.H. Hartwig, and T.P. Stossel. 2007. Structural basis of filamin A functions. 179:1011–1025. doi:10.1083/jcb.200707073.

Nakamura, F., T.P. Stossel, and J.H. Hartwig. 2011a. The filamins. *Cell Adh. Migr.* 5:160–169. doi:10.4161/cam.5.2.14401.

Nakamura, F., T.P. Stossel, and J.H. Hartwig. 2011b. The filamins Organizers of cell structure and function. *J. Cell Biol.* 5:160–169. doi:10.1083/jcb.200707073.

Oegema, K., M.S. Savoian, T.J. Mitchison, and C.M. Field. 2000. Functional analysis of a human homologue of the Drosophila actin binding protein anillin suggests a role in cytokinesis. *J. Cell Biol.* 150:539–551. doi:10.1083/jcb.150.3.539.

Ohta, Y., N. Suzuki, S. Nakamura, J.H. Hartwig, and T.P. Stossel. 1999. The small GTPase RalA targets filamin to induce filopodia. *Proc. Natl. Acad. Sci. U. S. A.* 96:2122–2128. doi:10.1073/pnas.96.5.2122.

Onoprishvili, I., M.L. Andria, H.K. Kramer, N. Ancevska-Taneva, J.M. Hiller, and E.J. Simon. 2003. Interaction Between the μ Opioid Receptor and Filamin A Is Involved in Receptor Regulation and Trafficking. *Mol. Pharmacol.* 64:1092–1100. doi:10.1124/mol.64.5.1092.

Ou, G., and R.D. Vale. 2009. Molecular signatures of cell migration in C. elegans Q neuroblasts. *J. Cell Biol.* 185:77–85. doi:10.1083/jcb.200812077.

Pollard, T.D., and C.C. Beltzner. 2002. Structure and function of the Arp2/3 complex. *Curr. Opin. Struct. Biol.* 12:768–774. doi:10.1016/S0959-440X(02)00396-2.

Pollard, T.D., and G.G. Borisy. 2003. Cellular Motility Driven by Assembly and Disassembly of Actin Filaments. *Cell*. 112:453–465.

Pollard, T.D., and J.A. Cooper. 2009. Actin, a Central Player in Cell Shape and Movement. *Science*. 326:1208–1212. doi:10.1126/science.1175862.

Pudas, R., T.R. Kiema, P.J.G. Butler, M. Stewart, and J. Ylänne. 2005. Structural basis for vertebrate filamin dimerization. *Structure*. 13:111–119. doi:10.1016/j.str.2004.10.014.

Raab, M., M. Gentili, H. de Belly, H.-R. Thiam, P. Vargas, A.J. Jiminez, F. Lautenschlaeger, R. Voituriez, A.-M. Lennon-Dumenil, N. Manel, and M. Piel. 2016. ESCRT III repairs nuclear envelope ruptures during cell migration to limit DNA damage and cell death. *Science (80-.).* 352:359–362.

Radisky, E.S., and D.C. Radisky. 2010. Matrix Metalloproteinase-Induced Epithelial-Mesenchymal Transition in Breast Cancer. *J. Mammary Gland Biol. Neoplasia*. 15:201–212. doi:10.1007/s10911-010-9177-x.

Rahman, M., I.Y. Chang, A. Harned, R. Maheshwari, K. Amoateng, K. Narayan, and O. Cohen-Fix. 2020. C. elegans pronuclei fuse after fertilization through a novel membrane structure. *J. Cell Biol.* 219. doi:10.1083/jcb.201909137.

Razinia, Z., T. Makela, J. Ylanne, and D.A. Calderwood. 2016. Filamins in mechanosensing and signaling. *Annu Rev Biophys*. 118:6072–6078. doi:10.1146/annurev-biophys-050511-102252.Filamins.

Reiner, D., and E.A. Lundquist. 2018. Small GTPases. *WormBook*. doi:10.1895/wormbook.1.67.2.

Roper, M., A. Simonin, P.C. Hickey, A. Leeder, and N.L. Glass. 2013. Nuclear dynamics in a fungal chimera. *P. Nat. Acad. Sci. USA*.

Sabin, F.R. 1928. Bone Marrow. *Physiol. Rev.* 8:191–244.

Salvermoser, M., D. Begandt, R. Alon, and B. Walzog. 2018. Nuclear deformation during neutrophil migration at sites of inflammation. *Front. Immunol.* 9:1–9. doi:10.3389/fimmu.2018.02680.

Schlüter, K., B.M. Jockusch, and M. Rothkegel. 1997. Profilins as regulators of actin dynamics. *Biochim. Biophys. Acta - Mol. Cell Res.* 1359:97–109. doi:10.1016/S0167-4889(97)00100-6.

Seyfried, T.N., and L.C. Huysentruyt. 2013. On the Origin of Cancer Metastasis. *Crit. Rev. Oncog.* 18:43–73.

Shakir, M.A., J.S. Gill, and E.A. Lundquist. 2006. Interactions of UNC-34 enabled with Rac GTPases and the NIK kinase MIG-15 in Caenorhabditis elegans axon pathfinding and neuronal migration. *Genetics*. 172:893–913. doi:10.1534/genetics.105.046359.

Shakir, M.A., K. Jiang, E.C. Struckhoff, R.S. Demarco, F.B. Patel, M.C. Soto, and E.A. Lundquist. 2008. The Arp2/3 Activators WAVE and WASP Have Distinct Genetic Interactions With Rac GTPases in Caenorhabditis elegans Axon Guidance. *Genetics*. 179:1957–1971. doi:10.1534/genetics.108.088963.

Sherwood, D.R., and P.W. Sternberg. 2003. Anchor Cell Invasion into the Vulval Epithelium in C . elegans. 5:21–31.

Shin, J.W., K.R. Spinler, J. Swift, J.A. Chasis, N. Mohandas, and D.E. Discher. 2013. Lamins regulate cell trafficking and lineage maturation of adult human hematopoietic cells. *Proc. Natl. Acad. Sci. U. S. A.* 110:18892–18897. doi:10.1073/pnas.1304996110.

Smith, A., Y.R. Carrasco, P. Stanley, N. Kieffer, F.D. Batista, and N. Hogg. 2005. A talin-dependent LFA-1 focal zone is formed by rapidly migrating T lymphocytes. *J. Cell Biol.* 170:141–151. doi:10.1083/jcb.200412032.

Sosa, B.A., A. Rothballer, U. Kutay, and T.U. Schwartz. 2012. LINC complexes form by binding of three KASH peptides to domain interfaces of trimeric SUN proteins. *Cell*. 149:1035–1047. doi:10.1016/j.cell.2012.03.046.

Soto, M.C., H. Qadota, K. Kasuya, M. Inoue, D. Tsuboi, C.C. Mello, and K. Kaibuchi. 2002. The GEX-2 and GEX-3 proteins are required for tissue morphogenesis and cell migranons in C. elegans. *Genes Dev.* 16:620–632. doi:10.1101/gad.955702.

Spencer, A.G., S. Orita, C.J. Malone, and M. Han. 2001. A RHO GTPase-mediated pathway is

required during P cell migration in Caenorhabditis elegans. *Proc. Natl. Acad. Sci. U. S. A.* 98:13132–13137. doi:10.1073/pnas.241504098.

Starr, D.A. 2019. A network of nuclear envelope proteins and cytoskeletal force generators mediates movements of and within nuclei throughout Caenorhabditis elegans development. *Exp. Biol. Med.* 244:1323–1332. doi:10.1177/1535370219871965.

Starr, D.A., G.J. Hermann, C.J. Malone, W. Fixsen, J.R. Priess, H.R. Horvitz, and M. Han. 2001. unc-83 encodes a novel component of the nuclear envelope and is essential for proper nuclear migration. *Development*. 128:5039–5050.

Stossel, T.P., J. Condeelis, L. Cooley, J.H. Hartwig, A. Noegel, M. Schleicher, and S.S. Shapiro. 2001. Filamins as integrators of cell mechanics and signalling. *Nat. Rev. Mol. Cell Biol.* 2:138–145. doi:10.1038/35052082.

Strome, S. 1986. Fluorescence Visualization of the Distribution of Microfilaments in Gonads and Early Embryos of the Nematode Caenorhabditis elegans. *J. Cell Biol.* 103:2241–2252.

Sulston, J.E., and H.R. Horvitz. 1977. Post-embryonic cell lineages of the nematode, Caenorhabditis elegans. *Dev. Biol.* 56:110–156. doi:https://doi.org/10.1016/0012-1606(77)90158-0.

Sulston, J.E., and H.R. Horvitz. 1981. Abnormal cell lineages in mutants of the nematode Caenorhabditis elegans. *Dev. Biol.* 82:41–55. doi:https://doi.org/10.1016/0012-1606(81)90427-9.

Sulston, J.E., E. Schierenberg, J.G. White, and J.N. Thomson. 1983. The embryonic cell lineage of the nematode Caenorhabditis elegans. *Dev. Biol.* 100:64–119. doi:10.1016/0012-1606(83)90201-4.

Sym, M., N. Robinson, and C. Kenyon. 1999. MIG-13 Positions Migrating Cells along the Anteroposterior Body Axis of C . elegans. 98:25–36.

Tan, P.Y., and R. Zaidel-Bar. 2015. Transient membrane localization of SPV-1 drives cyclical actomyosin contractions in the C elegans spermatheca. *Curr. Biol.* 25:141–151. doi:10.1016/j.cub.2014.11.033.

Theriot, J.A., and T.J. Mitchison. 1991. Actin microfilament dynamics in locomoting cells. 352.

Thiam, H.-R., P. Vargas, N. Carpi, C.L. Crespo, M. Raab, E. Terriac, M.C. King, J. Jacobelli, A.S. Alberts, T. Stradal, A.-M. Lennon-Dumenil, and M. Piel. 2016. Perinuclear Arp2/3-driven actin polymerization enables nuclear deformation to facilitate cell migration through complex environments. *Nat. Commun.* 7:10997. doi:10.1038/ncomms10997http://www.nature.com/articles/ncomms10997#supplementary-information.

Tian, D., M. Diao, Y. Jiang, L. Sun, Y. Zhang, Z. Chen, S. Huang, and G. Ou. 2015. Anillin Regulates Neuronal Migration and Neurite Growth by Linking RhoG to the Actin Cytoskeleton Article Anillin Regulates Neuronal Migration and Neurite Growth by Linking RhoG to the Actin Cytoskeleton. *Curr. Biol.* 25:1135–1145. doi:10.1016/j.cub.2015.02.072.

Ungricht, R., and U. Kutay. 2017a. Mechanisms and functions of nuclear envelope remodelling. *Nat. Publ. Gr.* 18. doi:10.1038/nrm.2016.153.

Ungricht, R., and U. Kutay. 2017b. Mechanisms and functions of nuclear envelope remodelling. *Nat. Rev. Mol. Cell Biol.* 18:229–245. doi:10.1038/nrm.2016.153.

Wallace, A.G., H. Raduwan, J. Carlet, and M.C. Soto. 2018. The RhoGAP HUM-7/myo9 integrates signals to modulate RHO-1/RhoA during embryonic morphogenesis in caenorhabditis elegans. *Dev.* 145. doi:10.1242/dev.168724.

Williams-Masson, E.M., A.N. Malik, and J. Hardin. 1997. An actin-mediated two-step mechanism is required for ventral enclosure of the C. elegans hypodermis. *Development*. 124:2889–2901. doi:10.1242/dev.124.15.2889.

Winder, S.J., and K.R. Ayscough. 2005. Actin-binding proteins. *J. Cell Sci.* 118:651–654. doi:10.1242/jcs.01670.

Wirshing, A.C.E., and E.J. Cram. 2017. Myosin activity drives actomyosin bundle formation and organization in contractile cells of the Caenorhabditis elegans spermatheca. *Mol. Biol. Cell*. 28:1937–1949. doi:10.1091/mbc.E17-01-0029.

Wissmann, A., J. Ingles, and P.E. Mains. 1999. The Caenorhabditis elegans mel-11 myosin phosphatase regulatory subunit affects tissue contraction in the somatic gonad and the embryonic epidermis and genetically interacts with the Rac signaling pathway. *Dev. Biol.* 209:111–127. doi:10.1006/dbio.1999.9242.

Withee, J., B. Galligan, N. Hawkins, and G. Garriga. 2004. Caenorhabditis elegans WASP and Ena / VASP Proteins Play Compensatory Roles in Morphogenesis and Neuronal Cell Migration. 1176:1165–1176. doi:10.1534/genetics.103.025676.

Wu, Y.C., T.W. Cheng, M.C. Lee, and N.Y. Weng. 2002. Distinct rac activation pathways control Caenorhabditis elegans cell migration and axon outgrowth. *Dev. Biol.* 250:145–155. doi:10.1006/dbio.2002.0785.

Xiong, H., W.A. Mohler, and M.C. Soto. 2011. The branched actin nucleator Arp2/3 promotes nuclear migrations and cell polarity in the C. elegans zygote. *Dev. Biol.* 357:356–369. doi:10.1016/j.ydbio.2011.07.008.

Yu, T.W., J.C. Hao, W. Lim, M. Tessier-lavigne, and C.I. Bargmann. 2002. Shared receptors in axon guidance : SAX-3 / Robo signals via UNC-34 / Enabled and a Netrin-independent UNC-40 / DCC function. doi:10.1038/nn956.

Zhu, Z., Y. Chai, Y. Jiang, W. Li, H. Hu, W. Li, J.W. Wu, Z.X. Wang, S. Huang, and G. Ou. 2016. Functional Coordination of WAVE and WASP in C. elegans Neuroblast Migration. *Dev. Cell*. 39:224–238. doi:10.1016/j.devcel.2016.09.029.

Zipkin, M.D., R.M. Kindt, and C.J. Kenyon. 1997. Role of a new Rho family member in cell migration and axon guidance in C. elegans. *Cell*. 90:883–894. doi:10.1016/S0092-8674(00)80353-0.

Chapter II: The divergent Filamin FLN-2 maintains nuclear integrity during P-cell nuclear migration through constrictions in *Caenorhabditis elegans*

Abstract

Cellular migration is important for many developmental processes, and the ability of a cell to migrate through constricted spaces may be linked to disease pathologies such as cancer metastasis. Often, cellular migration is limited by the ability of the nucleus to stably migrate through the constricted space. Our lab uses the nematode *Caenorhabditis* elegans as an *in vivo* model to study nuclear migration through constricted spaces In *C. elegans* larvae, 6 pairs of hypodermal P-cells migrate from the lateral to the ventral part of the worm through a constricted space 5% the diameter of the nucleus. These P-cells then divide and develop into the precursors to the GABA neurons and the vulva. Canonically, P-cell nuclear migration has been mediated by UNC-84 and UNC-83 using a microtubule-based pathway. However, studies have shown that P-cell nuclear migration at 15°C still occurs in the absence of UNC-84, but not at higher more restrictive temperatures. This suggested the presence of alternative enhancer pathways. Our lab previously conducted forward genetics screens and found Filamin-2 (FLN-2), as well as other putative actin-based players. In this work, we found that our *fln-2* isoform of interest lacks the N-terminal actin binding domain that canonical filamins posess. We used CRISPR to perform domain deletion analyses and found that *fln-2* Ig-like repeats 4-8 were important for P-cell nuclear migration. Further, FLN-2 did not appear to colocalize with actin either *in vivo* nor in U2OS cells. We also found that the absence of *unc-84* resulted in nuclear rupture and the absence of both *unc-84* and *fln-2* resulted in an increase of nuclear rupture.

Introduction

Cellular migration mediates developmental processes ranging from embryogenesis to neurodevelopment (Bone and Starr, 2016). Typically, migration through narrow spaces is limited by nuclear deformability, and the underlying mechanisms participate in immune response (i.e. white blood cells rushing to the site of injury), as well as metastatic processes (Barzilai et al., 2017; Seyfried and Huysentruyt, 2013). Unfortunately, metastatic invasion and proliferation is

the least understood area of cancer biology (Seyfried and Huysentruyt, 2013). *In vitro* studies show that metastatic cells can deform and migrate through PDMS-cast constrictions 5% of their original diameter (Thiam et al., 2016). Although these properties have been quantified *in vitro*, it is important to follow nuclear migration *in vivo* to delineate all the players.

Caenorhabditis elegans is an excellent *in vivo* model for studying nuclear migration through constricted spaces given our lab's prior track record in filming nuclear migration events and probing of the mechanisms which support this process (Bone et al., 2016; Chang et al., 2013). During development, *C. elegans* P-cells migrate through a narrow constriction from the lateral to the ventral part of the worm during the mid-L1 larval stage, where they then divide and form precursors to the vulva and GABA neurons (Sulston and Horvitz, 1977, 1981). If P-cell nuclear migration fails, the worm develops Egl (**eg**g-**l**aying deficient) and Unc (**unc**oordinated) phenotypes (Malone et al., 1999; Starr et al., 2001). Previous work in the lab suggests that P-cell nuclei deform during nuclear migration, however further work is needed to determine the exact nuclear dynamics during migration.

P-cell nuclear migration is typically facilitated by the SUN (Sad1 and UNC-84)-KASH (Klarsicht, ANC-1 and Syne Homology) microtubule-based pathway, where SUN proteins (UNC-84) recruit KASH proteins (UNC-83) to the nuclear envelope which then recruit microtubule motors (kinesin-1 and dynein) to coordinate nuclear migration. When either UNC-84 or UNC-83 is knocked out at 25°C, only 50% of P-cells successfully migrate. However, if the SUN-KASH pathway is knocked out at 15°C, 90% of P-cells successfully migrate (Chang et al., 2013; Sulston and Horvitz, 1981; Malone et al., 1999; Starr et al., 2001). This suggests an enhancer pathway is acting in parallel with the SUN-KASH-mediated pathway at 15°C.

We previously uncovered FLN-2 while screening for (*emus*) **e**nhancers of the nuclear **m**igration effect of **U**NC-84 (Chang et al., 2013). Given the role of canonical filamins as actin crosslinkers and bundlers (Gorlin et al., 1990; Gay et al., 2011), we propose that FLN-2 has an

actin-based role in mediating P-cell nuclear migration. We hypothesize that FLN-2 crosslinks branched actin present in the constriction to aid in stable nuclear deformation, and FLN-2 acts as an actin bundler to organize actin tracks behind the nucleus in preparation for actomyosin contraction which provides a force to mediate nuclear migration.

I am concentrating on FLN-2, a putative branched-actin crosslinker lacking the canonical N-terminus actin binding domain (ABD) of well-characterized filamins (Kovacevic and Cram, 2010). FLN-2 lacks the canonical calponin homology (CH) domain usually associated with actin binding/ bundling and cytolinking (Gimona et al., 2002). Therefore, it is unknown whether FLN-2 directly interacts with actin. Further, it lacks the dimerization domain that canonical filamins possess, and it is unknown if FLN-2 forms a dimer (DeMaso et al., 2011). Although FLN-2 is poorly conserved, many key features are conserved with mammalian filamins. Defects in mammalian filamins result in skeletal disorders such as otopalatodigital disorder (DeMaso et al., 2011). These conserved features include immunoglobulin (Ig)-like repeats, which facilitate protein-protein interactions. These Ig-like in human filamins are defined as two β sheets that form a β sandwich (Alzari, 1998). In this study, we take advantage of molecular tools to further probe FLN-2's Ig-like repeats and determine their role in mediating actin-based nuclear migration.

Methods

C. elegans strains and genetics

Animals were maintained on NGM plates spotted with colonies of OP50 and maintained at 15°C unless otherwise noted. We used *vab-10::mVenus2* (Kim et al., 2011)*; nls::TdTomato* (Spear and Erickson, 2012) under a P-cell specific *hlh-3* promoter (Doonan et al., 2008) wild-type worms(Chang et al., 2013) and crossed them into mutant backgrounds for our studies.

CRISPR/Cas9 mediated gene editing

The domain deletion analysis and the *fln-2c::spGFP11* animals were produced via CRISPR/Cas-9 microinjection (Paix et al., 2017, 2015; Farboud et al., 2019). Each animal was co-injected with *dpy-10* crRNA and ssODN repair template. The domain deletion analysis CRISPR worms used two crRNA guides and one ssODN repair template, while the *fln-2c::spGFP11* (spGFP11 sequence from (Cabantous et al., 2005)) worm used one crRNA guide and one ssODN repair template. crRNA guides and ssODN repairs can be found in **Table 2.2**. Injection mixes were prepared as follows: 0.2ul of *dpy-10* crRNA (8µg/ul) (Dharmacon/ Horizon Discovery), a total of 1.5ul of the target gene crRNA (4µg/ul) (0.75ul of each guide if there are two guides) (Dharmacon/ Horizon Discovery), 1.9ul of tracrRNA (4µg/ul) (Dharmacon/ Horizon Discovery), 0.525ul of *dpy-10* ssODN, 1.1ul of the target gene (1µg/ul), 4ul of Cas9 (10µg/ul) (UC Berkeley QB3), and 0.78ul of H2O. The injection mix was then injected into the gonads of young adult hermaphrodite animals. *fln-2c(ΔIg4-9)]X, fln-2c(ΔIg9-15)]X, fln-2c(Δ15-23)]X,* and *[spGFP11::fln-2c]X* ssODN (manufactured by Integrated DNA Technologies) repair templates were used.

mos1-mediated single copy insertion(mosSCI)

UD593 was created by amplifying *phlh-3, lifeact,* and *mKate2* from pSL780 (Riedl et al., 2008; Bone et al., 2016), then each gene was BP Gateway cloned into three different entry clones (pDONR 221 P4-P1R, pDONR 221, and pDONR 221 P2r-P3, respectively ThermoFisher Scientific #12536017), and LR Gateway cloned into the pCFJ150 targeting vector (a gift from Erik Jorgensen (Addgene plasmid # 19329 ; http://n2t.net/addgene:19329 ; RRID:Addgene_19329) (Frøkjær-Jensen et al., 2008) and named pSL831*([phlh-3::lifeact::mKate2]II, pCFJ150[unc-119(+)].* This plasmid was injected into the gonad of young adult hermaphrodite EG6699 (*ttTi5605)* worms (Frøkjær-Jensen et al., 2012) along with co-injection markers pCFJ601 *(Peft-3* Mos1 transposase) (50ng/ul), pMA122 (*peel-1* negative

selection) (10ng/ul), pGH8 (*Prab-3::mCherry)* (10ng/ul), pCFJ90 *(Pmyo-3::twk-18(cn110))* (2.5ng/ul), pCFJ104 *(Pmyo-3::mCherry)* (5ng/ul) (Frøkjær-Jensen et al., 2008, 2012). These injected animals were maintained on HB101 plates at 25C until completely starved and heat shocked at 34C for two hours, we then looked for worms, using our Leica fluorescent dissecting microscope, which moved like wildtype and lacked the red co-injection markers. This single copy insertion of pSL831 was then named ycSI1.

We then created pSL832 *[phlh-3::nls::gfp lacZ]* by amplifying nls::gfp::LacZ from pPD96.04 (a gift from Andrew Fire, Addgene plasmid # 1502 ; http://n2t.net/addgene:1502 ; RRID:Addgene_1502) and inserting this into a pSL780 backbone (*phlh-3::lifeact::mKate2)*, replacing the *lifeact::mKate2* with our *nls::gfp::lacZ*. This plasmid was microinjected into the germline of young adult hermaphrodite UD593 worms to create UD614 (*ycEx283[10ng/ul phlh3::nls::gfp::lacZ, 90ng/ul odr-1::gfp] ycSi1[phlh3::lifeact::mKate2]II).*

Assays for quantifying nuclear migration defect

Animals were microinjected with an *unc-47::GFP* marker to assay the number of GABA neurons present in young adult worms (McIntire S. L. Schuske K., Edwards R. H., Jorgensen E. M., 1997). Refer to Method 3.3 (Fridolfsson et al., 2018) for more detail about the assay. We conducted this assay in young adult worms as a proxy for determining how many P cells successfully migrated in the L1 stage, as it has proven difficult to watch P cell migration occur in real time.

Actin Colocalization Experiment

I PCR amplified the first 5 Ig-like repeats of *fln-2c* insert from FLN-2C cDNA and the backbone from the SC444 (GFP-CMV) (a gift from the lab of Sean Collins, UC Davis) plasmid, I then used Gibson assembly (NEB# E2611L) to create pSL849. I transiently expressed pSL849 in U2Os cells at 500ng/ul overnight and washed with PBS prior to fixation. I fixed U2OS cells for 15 minutes with methanol-free 4% formaldehyde and rinsed three times in PBS for 5 minutes

each. 0.33μM of phalloidin Alexa 647 (Cell Signaling Technology #8940) and 0.3μM DAPI were incubated to stain the actin and nuclei. Following fixation and incubation, these cells were imaged on the Zeiss LSM 980 with Airyscan.

Microscopy and Synchronization

To prepare *C. elegans* L1 worms undergoing P-cell nuclear migration, we begun this process 18 hours prior to the imaging event. Six gravid plates of hermaphrodites were bleached (Stiernagle, 2006). We collected three plates in total, then we allowed the embryos we collected to grow at 15°C, 18°C, and 20°C for 18 hours. This allows us to have animal populations undergoing pre-, mid-, and post-migration.

To prepare slides, one hour prior to imaging, we screened under our fluorescent dissecting scope to determine which stage of migration our plates are in by looking at *phlh-3::nls::tdTomato* P-cell nuclear marker. Making sure to heat up VALAP (Equal parts Vaseline, Lanolin, and Paraffin mixture) so it will be ready to use after slides are done. We made 2% agarose pad slides (Fridolfsson et al., 2018) and reserved these to be used later. We then prepared slides based on the varying stages of P-cell nuclear migration. Plates of animals were washed with 2mL of M9 buffer, which were collected into 2mL microcentrifuge tubes. We spun briefly with the pulse setting on our microcentrifuge (Thermo Scientific Sorvall Legend Micro 17 microcentrifuge), discarded the supernatant (taking care not to disturb the worm pellet), and added 1mL of M9 buffer to the microcentrifuge tube. We then spun briefly, to try and clear out as much OP50 as possible and vacuumed the supernatant until we had about 20μl of supernatant left and the worm pellet was intact.

We then mixed up and down with a pipet briefly to break up the worm pellet and transferred the contents of each microcentrifuge tube to the 2% agarose pad slides we prepared earlier. We added an equivalent amount of 2μM tetramizole (for a final concentration of 1μM tetramizole) to the slides and allowed to air dry before covering with a coverslip. Once this was

complete, we sealed each slide with VALAP and created a humidity chamber in our slide box with a wet tissue or kimwipe.

We imaged these slides on a Zeiss LSM 980 with Airyscan and with the 63x oil objective, using the 561nm and 488nm lasers. Images were acquired with the Zeiss Zen Blue software. They were processed through the Zeiss Airyscan filter and then further examined using FIJI.

Results

2.1 FLN-2 is an enhancer of the nuclear migration defect of *unc-84*

Our lab previously performed a screen to identify *enhancers of the nuclear migration defect of unc-84* (*emu*). These *emu* genes function in parallel pathways to LINC complexes during P-cell nuclear migration (Chang et al., 2013). While analyzing mutant alleles from that screen, we found that mutants in *fln-2* also enhance the nuclear migration defect of *unc-84* (Fig 1e). After screening for *emus*, we conducted a secondary GABA neuron assay following the *unc-47::gfp* marker to ensure that any candidates are indeed *emu*s (Chang et al., 2013) (**Fig 2.1a-c, e**). Following successful P-cell nuclear migration, the worm develops 19 GABA neurons in wild-type adults, 12 of which are P-cell derived (Sulston and Horvitz, 1977). The maximum amount of missing GABA neurons resulting from P-cell nuclear migration failure is 12. We use broodmates as controls when scoring GABA neurons; lines containing extrachromosomal arrays with genomic DNA covering *unc-84* and/or *fln-2* that rescue mutants and are marked with fluorescent tags allowing us to perform blind GABA neuron counts. *fln-2* (an average of 2.4 missing GABA neurons) and *unc-84* (an average of 1.1 missing GABA neurons) single mutants exhibit minimal GABA neuron loss at the permissive temperature, while the *fln-2(tm4687) unc-84(n369)* double mutant animals were missing significantly more GABA neurons than the single mutants (an average of 6.6 missing GABA neurons) (**Fig 2.1e**). Therefore, the *unc-84; fln-2*

double mutant enhances the nuclear migration defect of *unc-84*, suggesting FLN-2 has a role in P-cell nuclear migration.

There are 22 predicted *fln-2* isoforms from multiple start and termination sites as well as alternative splice sites; 4 are shown in Figure 1d (wormbase.org) (DeMaso et al., 2011). We performed genetic analyses to determine which *fln-2* isoforms are necessary for P-cell nuclear migration. The *fln-2(tm4687)* allele, which has a 547 bp deletion in the 3' half of the gene, is predicted to disrupt most FLN-2 isoforms and caused a strong nuclear migration defect (**Fig 2.1**). In contrast, the *fln-2(ot611)* mutant, which introduces an early stop codon in only the longer isoforms, was found in our background strain, UD87, that was used for our enhancer screen. Therefore, the *ot611* allele has no phenotype, suggesting that the longer isoforms are not necessary for P-cell nuclear migration. We used the Ahringer RNAi library (Fraser et al., 2000; Kamath et al., 2003) at 15°C to target a region downstream (X-4P01) of *ot611* and found a significant phenotype in *fln-2(RNAi) unc-84(n369)* animals (an average of 4.55±2.2 missing GABA neurons compared to only 1.1±0.8 missing GABA neurons in untreated *unc-84(n369)* animals) (**Fig 2.1e**). We then turned our attention to the *fln-2(tm4687)* deletion (an average of 6.6±1.8 missing GABA neurons) and found that this enhanced the nuclear migration defect of wild-type animals (**Fig 2.1e**).

We then performed fosmid rescue experiments in *fln-2(tm4687) unc-84(n369)* animals (**Fig 2.1d, f, g**). We found that a combination of two fosmids (WRM0625cB05 and WRM0620dC04) that span the entire *fln-2* locus rescued the *fln-2(tm4687) unc-84(n369)* P-cell nuclear migration defect. Furthermore, a shorter fosmid, WRM0625cB05 (Tursun et al., 2009), that did not include the longer *fln-2* isoforms was also able to rescue the *fln-2(tm4687) unc-84(n369)* P-cell nuclear migration defect, supporting our model where only the smaller isoforms related to *fln-2c* and *fln-2d* are necessary for P-cell nuclear migration (**Fig 2.1f, g**). In support of this model, it was previously determined that *fln-2a* and *fln-2b* are expressed primarily during embryogenesis, while *fln-2c* and/or *fln-2d* are expressed at later stages, including L1 larvae

(DeMaso et al., 2011). The *fln-2c* and *fln-2d* isoforms do not contain the N-terminal actin-binding domain found in the longer isoforms and canonical filamin homologs. It is therefore unclear whether FLN-2 interacts with actin (directly or indirectly).

2.2: Actin plays a role in mediating nuclear migration through narrow constrictions

We previously determined that P-cell nuclei undergo gross morphological changes as they migrate through a constriction as narrow as 5% of their resting width in the mid-L1 stage (Bone et al., 2016). Our studies indicate that these changes are dependent on dynein working through LINC complexes and at least one additional pathway uncovered in our forward genetic screen for enhancers of mutations in LINC complexes (Chang et al., 2013; Bone et al., 2016; Ho et al., 2018). The Piel group investigated how mouse dendritic cells (DCs) can migrate through small constrictions in an *in vitro* system. They induced mouse dendritic cells (DC) to migrate through 1µm constrictions (approximately 14% of the DC diameter), and found only 4% of DCs successfully migrated. They uncovered that Arp2/3-driven actin polymerization permitted nuclear deformation when the nuclei successfully migrated at less restrictive constrictions (Thiam et al., 2016). This, paired with our discovery of the putative actin player, FLN-2, led us to hypothesize that actin networks play important roles in P-cell nuclear migration, given that filamins canonically act to crosslink and bundle actin networks. However, it is not known what actin's role is in facilitating this process or how actin networks are organized throughout P-cell nuclear migration.

To better understand the organization of actin networks in larval P cells, we expressed both *vab-10::mVenus* (Kim et al., 2011; Bone et al., 2016) to mark actin filaments and *nls::tdTomato* to mark P-cell nuclei under the control of the P-cell-specific *hlh-3* (Chang et al., 2013; Doonan et al., 2008; Bone et al., 2016; Köppen et al., 2001) promoter in wild-type animals. As an alternative to the *vab-10::mVenus* actin marker, I expressed *lifeact::mKate2* (Riedl et al., 2008) under a P-cell-specific *hlh-3* promoter as a single-copy transposon inserted

into a known locus (*ttTi5605*) in the genome using *mosSCI* (Frøkjær-Jensen et al., 2014). Both the over-expressed *vab-10::mVenus* (actin in **Fig 2.2a**) and the single-copy *lifeact::mKate2* (actin in **Fig S2.1a**) markers appeared to localize in similar patterns when imaged with Airyscan super-resolution microscopy. However, the *nls::GFP* marker in the single-copy *lifeact::mKate2* strain was leaky (**Fig S2.1a**), likely due to its small size compared to *nls::tdTomato*. We therefore focused on using the *vab10::mVenus* marker strain.

We focused on the narrowing and migration stages of P-cell nuclear migration. A cartoon of the ventral view is shown in **Fig 2.2b**, and the lateral view is in **Fig 2.2c.** During the narrowing stage, the most anterior pair of P cells (cyan in **Fig 2.2b, c**) narrows first, with the most posterior pair narrowing last. Once migration begins, the most anterior pair of P cells will migrate under the muscle (transparent grey bar in **Fig 2.2b, c**) to the ventral cord (dashed line in **Fig 2.2b, c**) first and most posterior pair will complete migration last. P cell migration will not complete until the nuclei (magenta in **Fig 2.2b, c**) move from the lateral compartment to the ventral cord (**Fig 2.2b, c**).

We found that actin was present both behind the nucleus (orange arrow in inset of **Fig 2.2a**) and in the constriction (white arrow in inset of **Fig 2.2a**) during mid P-cell nuclear migration using live Airyscan imaging in 16 out of 16 worms. **Figure 2.2a** shows six pairs of P-cell nuclei migrating toward the ventral cord (indicated by the dashed white line), the first pair has already migrated while the second, third, and fourth pairs are migrating, and the last two pairs have not yet migrated. We frequently observed large actin bundles forming perpendicular to the direction of nuclear migration in the lateral part of P cells that were associated with the rearward parts of migrating nuclei (orange arrows in **Fig 2.2a**). Additionally, we observed actin fibers forming parallel to the direction of nuclear migration within the constriction (white arrows in **Fig 2.2a**). These data suggest actin localizes in the lateral part of the P-cell and the constriction prior to and during P-cell nuclear migration.

We next wanted to compare how actin may look in the wild-type and mutant animals. Actin's architecture in wild-type and mutant (*unc-84(n369)*, *fln-2(tm4687)*, and *fln-2(tm4687) unc-84(n369)*)animals appeared similar and did not have any gross changes from the wildtype (**Fig 2.2d**). All images are captured during mid-migration, with the ventral cord represented by the dashed line.

2.3: The domain of FLN-2 involved in P-cell nuclear migration is either Ig-like repeats 4, 5, 6, 7, 8, or some combination

We determined that *fln-2c* was our isoform of interest. As none of the short isoforms (*fln-2c* included) have the N-terminal actin-binding domain, we then performed CRISPR/Cas9-mediated domain deletions to determine which FLN-2 Ig-like repeats were involved with P-cell nuclear migration. We will henceforth refer to these Ig-like repeats as Ig-repeats. *fln-2c* consists of 2776 amino acids and has 20 Ig repeats, so we divided these into three overlapping segments (Ig 4-9, Ig 9-15, and Ig 15-23) (**Fig 2.3a**). We begin numbering with Ig4, as *fln-2a* is the full-length isoform containing calponin homology domains and Ig1-23.

We found that Ig 4-9 were necessary in P-cell nuclear migration (**Fig 2.3b)**, while Ig 9-23 were not (**Fig 2.3c, d**). We further quantified the severity of the nuclear migration defect by performing GABA neuron counts at the non-permissive temperatures of 20°C, and 25°C (**Supp. Fig. 2.2A-F**). Given that the loss of Ig9 through our Ig9-15 deletion did not significantly affect P-cell nuclear migration, we believe that *fln-2* Ig4-8 is necessary for P-cell nuclear migration.

2.4 P-cell nuclei in mutants rupture post-migration

While imaging our wildtype and mutant animals at varying stages of nuclear migration, we observed frequent nuclear rupture events in our mutants (*unc-84(n369), fln-2(tm4687), and fln-2(tm4687) unc-84(n369)*) (**Fig 2.4a**). Nuclear signal was dilute and localized to both the lateral and ventral compartments of the P-cell. We found that the number of post-migration

nuclear rupture events were significant in the *unc-84(n369)* single mutant (N=15), but not in *fln-2(tm4687)* single mutants (N=19). In addition, *fln-2(tm4687)* enhanced the nuclear rupture phenotype of *unc-84(n369)* in the double mutant (N=28) (**Fig 2.4b**). These ruptured nuclei persist while neighboring non-ruptured nuclei divide, though fluorescent signal is found in the ventral part of the worm. However, these ruptured nuclei persist into the late L1-larval stage.

2.5 FLN-2 does not colocalize with actin, but does surround the nucleus

Given that canonical filamins directly interact with actin, we wanted to determine whether *fln-2* Ig4-8 would colocalize with actin *in vitro*. We expressed *fln-2* Ig4-8::*gfp* under a CMV promoter in U2OS cells, and stained for DAPI and phalloidin Alexa 647. They did not colocalize with actin, but did appear to colocalize with the DAPI marker (n=24) in circular regions approximately 2.5 μm in size. (**Fig 2.5a**). We then examined how FLN-2c would behave *in vivo*, and expressed *spGFP::fln-2c* in L1 animals under a P-cell specific promoter and found that it localized to the nucleus and appeared in the constriction as well (**Fig 2.5b**), We next wanted to determine whether this spGFP tag disrupted FLN-2 function, and crossed this strain into our *unc-84(n369) unc-47::GFP* strain to count the number of missing GABA neurons. We found that there were no significant differences in the number of GABA neurons between the worms with and without the spGFP tag (**Fig 2.5c**).

Discussion

Microtubules have canonically served as the cytoskeletal tracks facilitating *C. elegans* P-cell nuclear migration through the SUN-KASH / LINC complex pathway. This pathway is where the SUN protein UNC-84 (on the inner nuclear membrane) recruits the KASH protein UNC-83 to the outer nuclear membrane which then recruits microtubule motors (kinesin-1 and cytoplasmic dynein) which bind to microtubule-associated proteins which facilitates nuclear migration along the microtubules (Ho et al., 2018; Bone et al., 2016; Starr et al., 2001). Our lab has previously shown that actin plays a role in a parallel pathway to mediate P-cell nuclear migration through

putative actin players (Bone et al., 2016; Chang et al., 2013). Though the mechanisms facilitating this pathway were not yet known. In this study, we show Filamin-2's role in mediating nuclear migration through narrow constrictions.

Without FLN-2's participation in P-cell nuclear migration, nuclear rupture occurs much more frequently, and especially so in the absence of UNC-84. Upon knocking out *unc-84(n369)* and *fln-2(tm4687)*, we found that there were ruptured nuclei in late-L1 animals. We theorize that the actin-based pathway may assist to stably deform the nuclei during migration. In the absence of the actin-based pathway and the microtubule-based pathway, these nuclei either rupture or fail to migrate and subsequently fail to divide and form the GABA neurons and vulva. Given the Egl and Unc phenotypes of *unc-84(n369); fln-2(tm4687)* worms, we speculate that P-cell death may be occurring upon rupture. Further investigation can be conducted with the microfluidic chip from our collaborators in Switzerland (Berger et al., 2021), where an L1 larvae can be filmed from the onset of P-cell nuclear migration until the young adult stage where the GABA neurons will finish developing.

FLN-2C does not possess the N-terminal actin binding domain that canonical filamins use to interact with actin. Upon closer inspection via domain deletion analysis, we found that Ig4-8 were involved in P-cell nuclear migration. We then transiently expressed these five repeats in U2OS cells and upon staining with phalloidin and DAPI found that they did not interact with actin in mammalian cell culture. We are unsure whether this is due to FLN-2 actually not interacting directly with actin, improper folding due to the absence of Ig9-15 or incompatibility of expressing a worm protein in a mammalian cell line. We did find that the FLN-2 signal seemed to be nucleoplasmic.

Figures

Figure 2.1 FLN-2 is an enhancer of the nuclear migration defect of *unc-84*

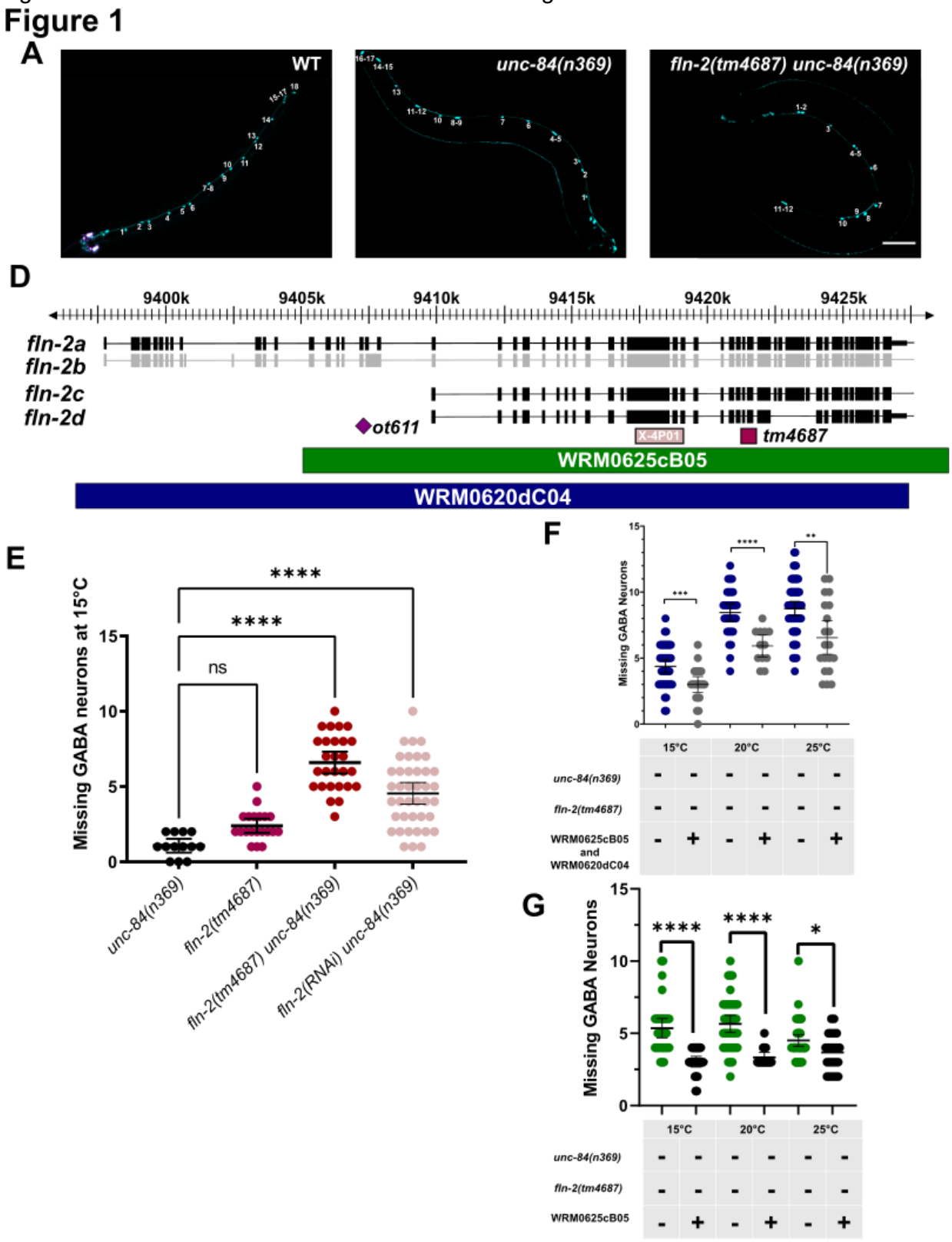

Figure 2.1: FLN-2 is an enhancer of the nuclear migration defect of *unc-84*

GABA neurons expressed via an *unc-47::gfp* marker in a **A)** wild-type animal, **B)** *unc-84(n369)* animal, **C)** *unc-84(n369); fln-2(tm4687)* animal **D)** Schematic of the introns and exons of four of the twenty-two known isoforms of FLN-2 indicated in black. Purple box indicates the *ot611* point mutant producing an early stop and encompassing the longer isoforms of FLN-2. The light pink box indicates the X-4P01 Ahringer RNAi targeting shorter isoforms of FLN-2. The magenta box shows the location of the tm4687 allele. The green box indicates the location of the short fosmid (WRM0625cB05), and blue box indicates the location of the long fosmid (WRM0620dC04). The gray boxes indicate that FLN-2B is a non-coding isoform. **** signifies a P-value < 0.0001 **E)** The missing GABA neuron assay counts with *unc-84(n369)* in black, *fln-2(tm4687)* in magenta, *unc-84(n369); fln-2(tm4687)* double mutant in red, and the *unc-84(n369); fln-2(X-4P01)* RNAi in light pink. **F)** The missing GABA neuron counts for the *unc-84(n369); fln-2(tm4687)* in dark blue and the double mutant with a long and short fosmid rescue in grey at the permissive temperature of 15°C and the restrictive temperatures of 20°C and 25°C. ** indicates a P-value of 0.0025, *** indicates a P-value of 0.0007, and **** indicates a P-value < 0.0001 **G)** The missing GABA neuron counts for the *unc-84(n369); fln-2(tm4687)* in green and the double mutant with a short fosmid rescue in black at the permissive temperature of 15°C and the restrictive temperatures of 20°C and 25°C. * indicates a P-value of 0.0196 and **** indicates a P-value < 0.0001

All error bars are 95% confidence intervals.

Figure 2.2 Actin plays a role in mediating nuclear migration through narrow constrictions

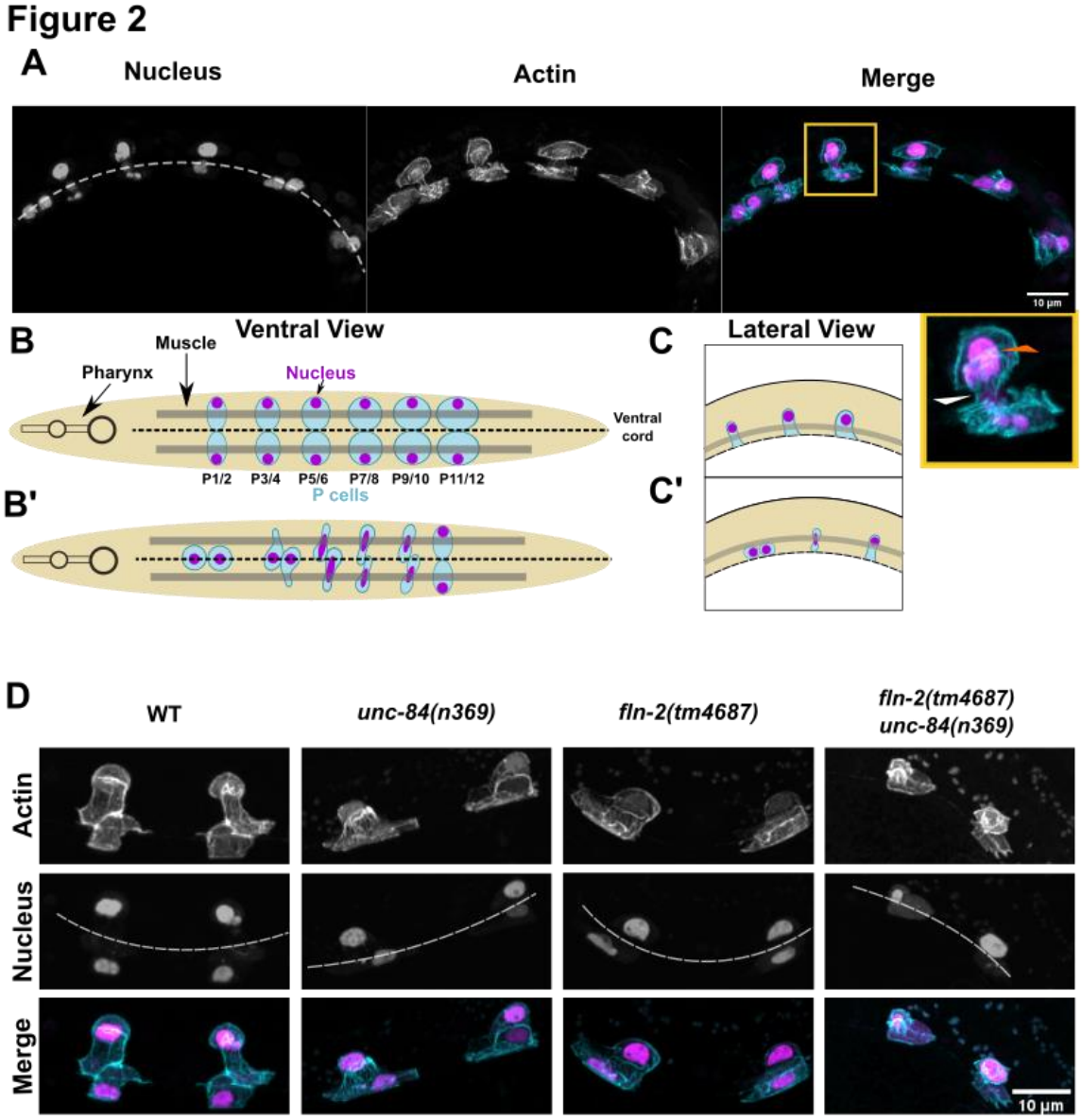

Figure 2.2: Actin plays a role in mediating nuclear migration through narrow constrictions

We tagged the actin (*vab-10::mVenus*) and P-cell nuclei (*nls::tdTomato*) in wild-type worms to observe their structure during migration. The gold box is around a migrating P cell in the merged channel. In the gold inset, the orange arrow indicates actin bundles in the lateral compartment, and the white arrow indicates actin in the constriction. The scale bar indicates 10 microns. **B, C**) A ventral view (**B**) and lateral view (**C**) of P cells during the narrowing and

migration stages. P cells are in cyan, nuclei are in magenta, the dashed line indicates the ventral cord. The pharynx indicates the most anterior point of the worm. The muscles are represented by the transparent gray bar overlaying the P cells. **D**) Actin (*vab10::mVenus*) and P-cell nuclei (*nls::tdTomato*) in wild-type, *unc-84(n369)*, *fln-2(tm4687)*, and the *fln-2(tm4687) unc-84(n369)* double mutant. The scale bar indicates 10 microns.

Figure 2.3 The domain involved in P-cell nuclear migration is either Ig-like repeats 4, 5, 6, 7, 8, or some combination

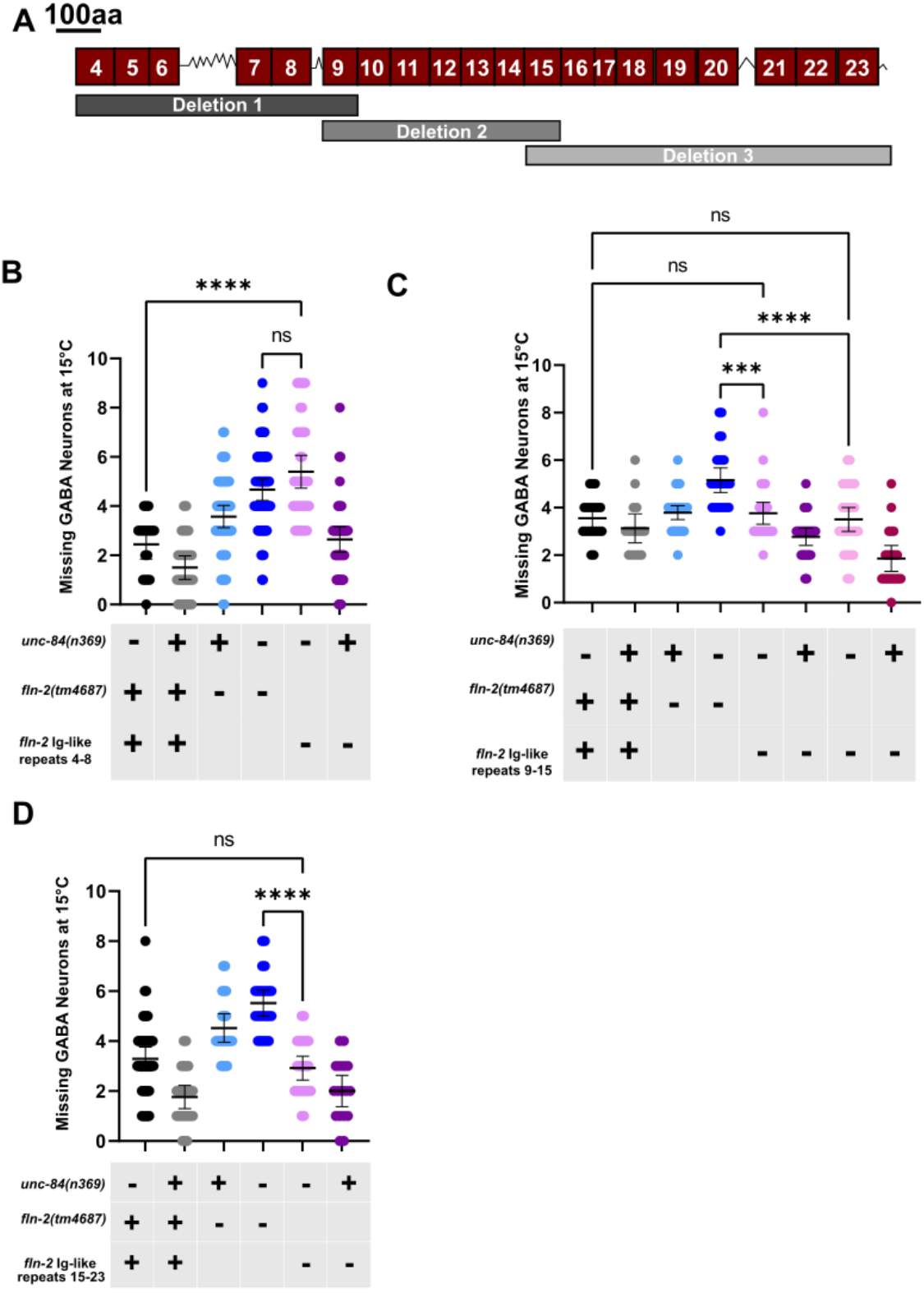

Figure 2.3: The domain involved in P-cell nuclear migration is either Ig-like repeats 4, 5, 6, 7, 8, or some combination

The red boxes indicate the Ig-like repeats of fln-2c, the disordered regions are indicated by the zig-zag lines, and the corresponding three deletions to 3B, C, D are shown by deletion 1, 2, 3 in varying grey boxes. The scale bar indicates 100 amino acids. B-D) Missing GABA neurons counted at 15°C for deletion 1 (B), deletion 2 (C), and deletion 3 (D). *** indicates p-value of 0.0003, **** indicates a p-value < 0.0001, all error bars are 95% confidence intervals and a one-way ANOVA test was done to generate p-values.

Figure 2.4 P-cell nuclei in mutants rupture post-migration

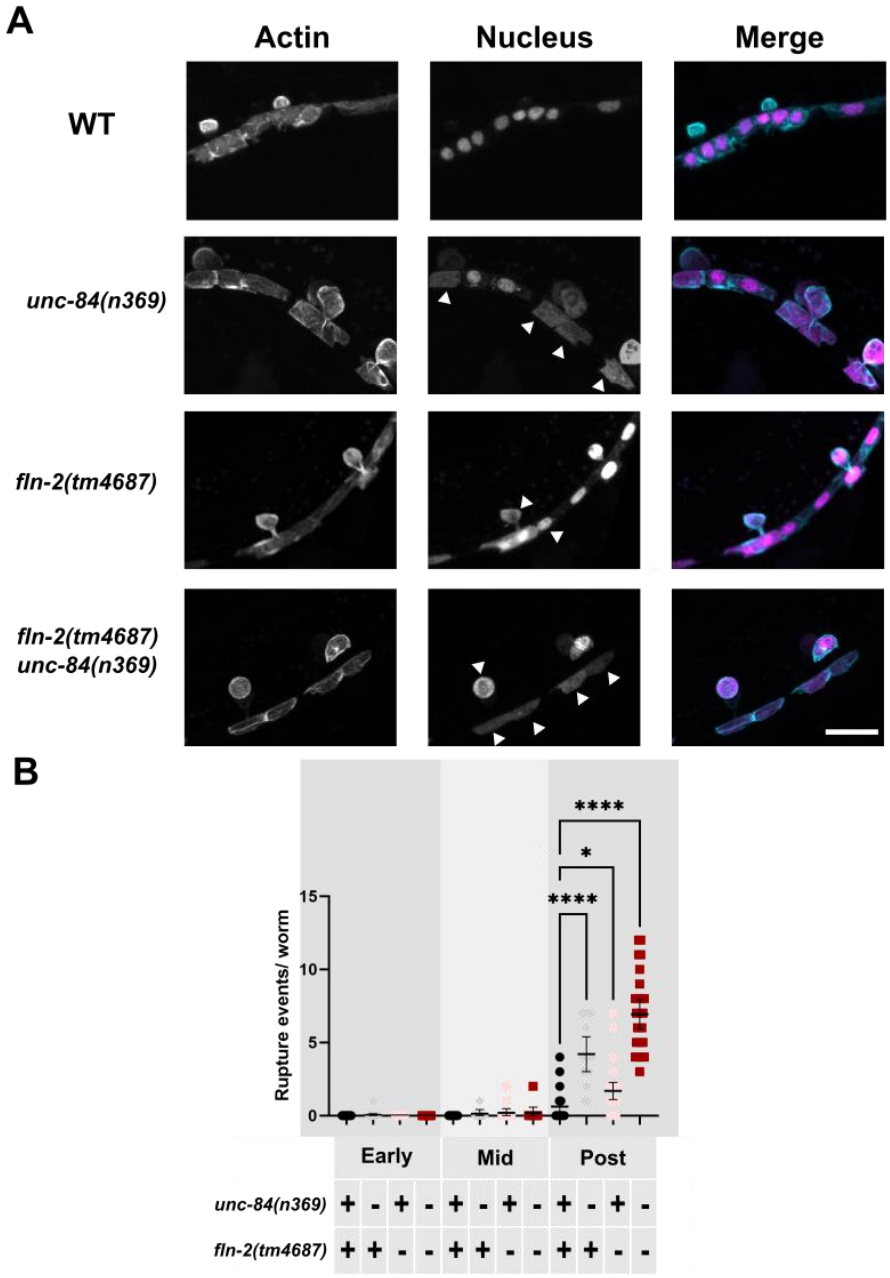

Figure 2.4 P-cell nuclei in mutants rupture post-migration

A) Late P-cell nuclear migration in WT, *unc-84(n369)*, *fln-2(tm4687)*, and *fln-2(tm4687) unc-84(n369)* animals. Scale bar is 10μm. Arrows point to suspected nuclear rupture events. **B)** Rupture events per worm in late stage nuclear migration. Error bars are 95% CI and **** denotes a p-value of <0.00001.

Figure 2.5 FLN-2 does not colocalize with actin, but does surround the nucleus

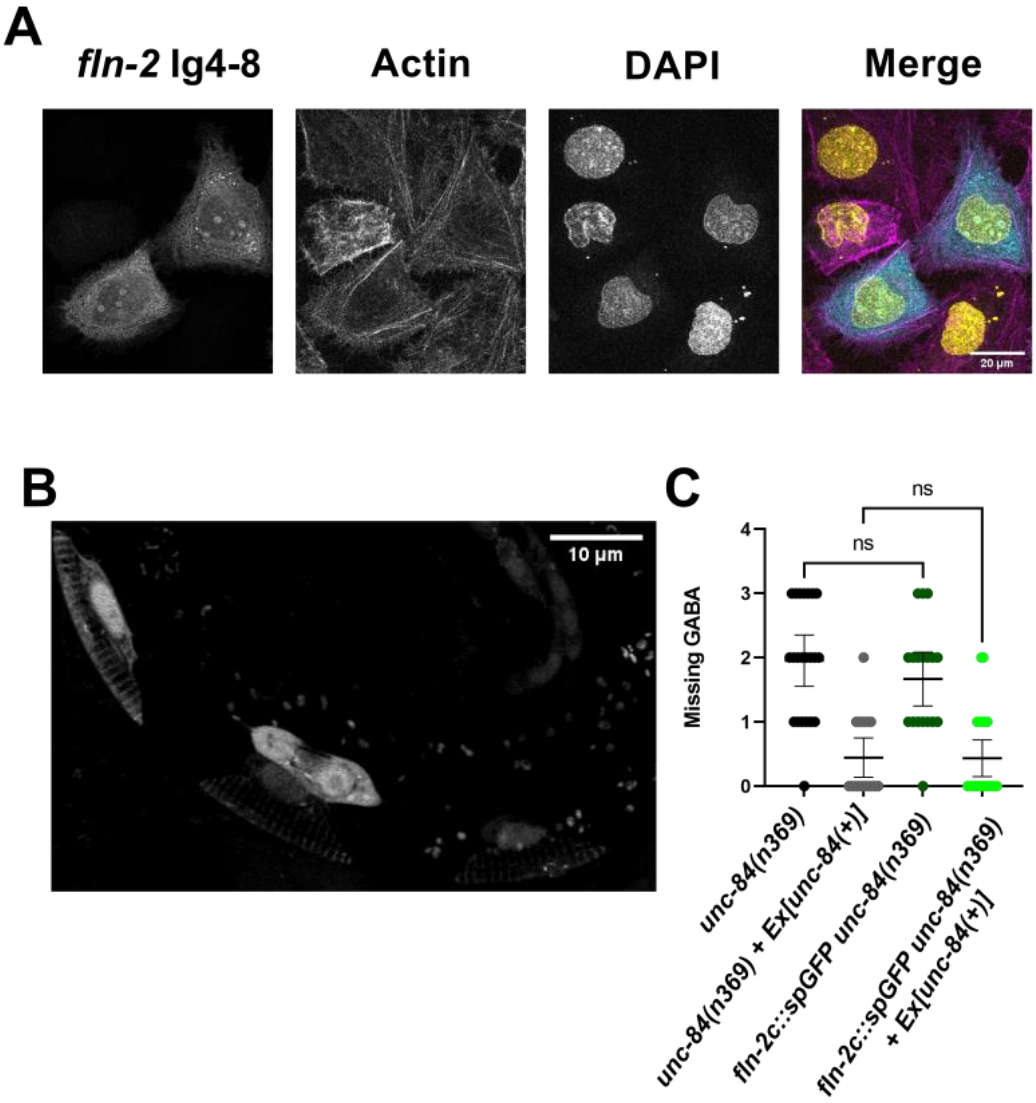

Figure 2.5 FLN-2 does not colocalize with actin, but does surround the nucleus.

A) *fln-2* Ig4-8::*gfp* transiently expressed in U2OS cells, stained with phalloidin Alexa647, and DAPI. **B)** *fln-2c::GFP* expressed in a *C. elegans* worm. **C)** Graph depicting the number of missing GABA neurons in *unc-84(n369)*, *unc-84(n369) + Ex[unc-84(+)]*, *fln-2c::spGFP unc-84(n369)*, and *fln-2c::spGFP unc-84(n369) + Ex[unc-84(+)]* worms. Error bars are 95% CI, and non-significant P-values > 0.05.

Supplemental Figures

Supplemental Figure 2.1 The mosSCI *lifeact::mkate2* labeled actin has similar expression to the *vab-10::mVenus* strain, while the *nls-lacZ::gfp* was leaky and the *nls::tdtomato* was not

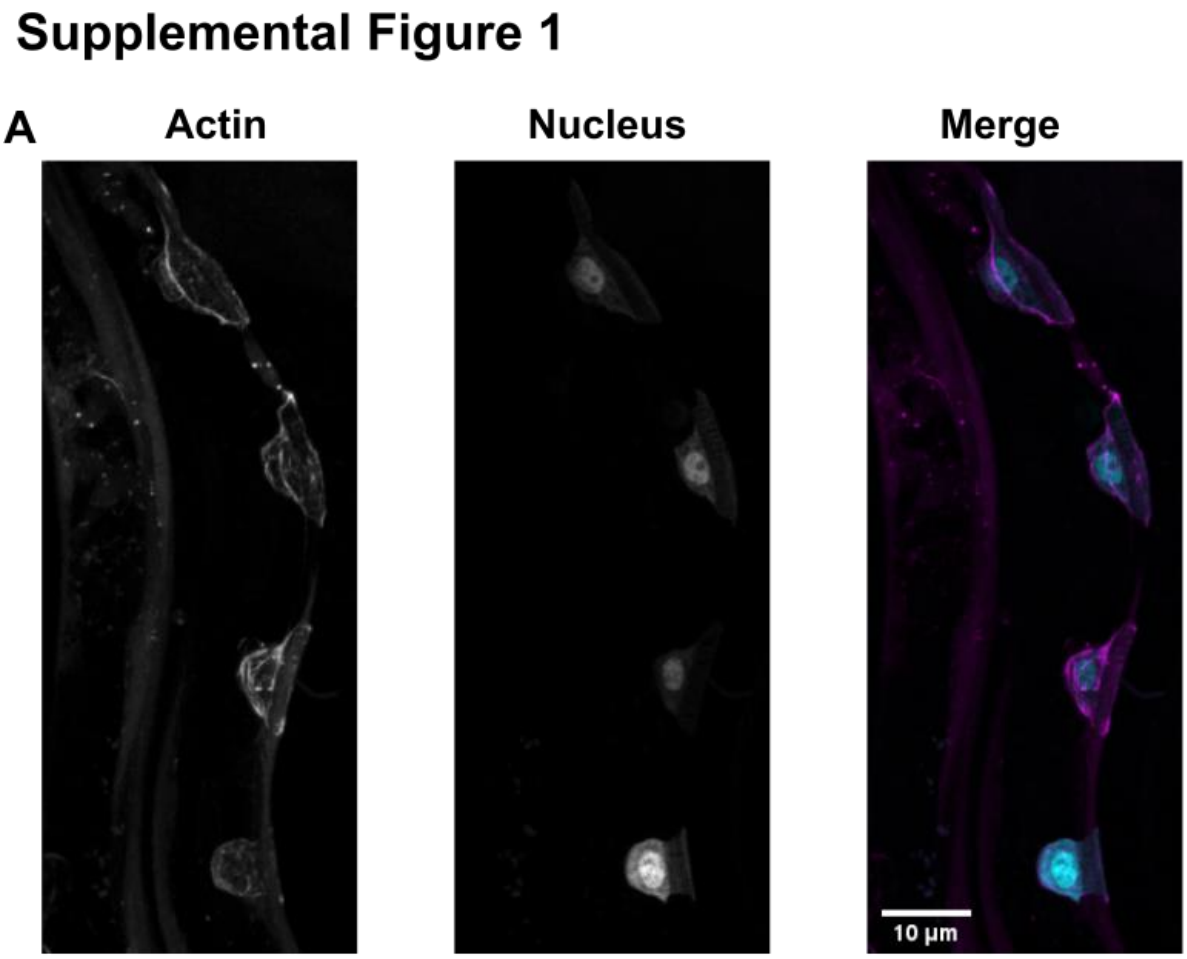

Supplemental Figure 1 The mosSCI *lifeact::mkate2* labeled actin has similar expression to the *vab-10::mVenus* strain, while the *nls-lacZ::gfp* was leaky and the *nls::tdtomato* was not

A) The nuclear signal in our MosSCI actin strain was leaky. The actin and nuclear channels are shown along with the merged image.

Supplemental Figure 2.2 FLN-2 Ig 4-8 are important in the restrictive temperatures, while Ig9-23 are not

Supplemental Figure 2

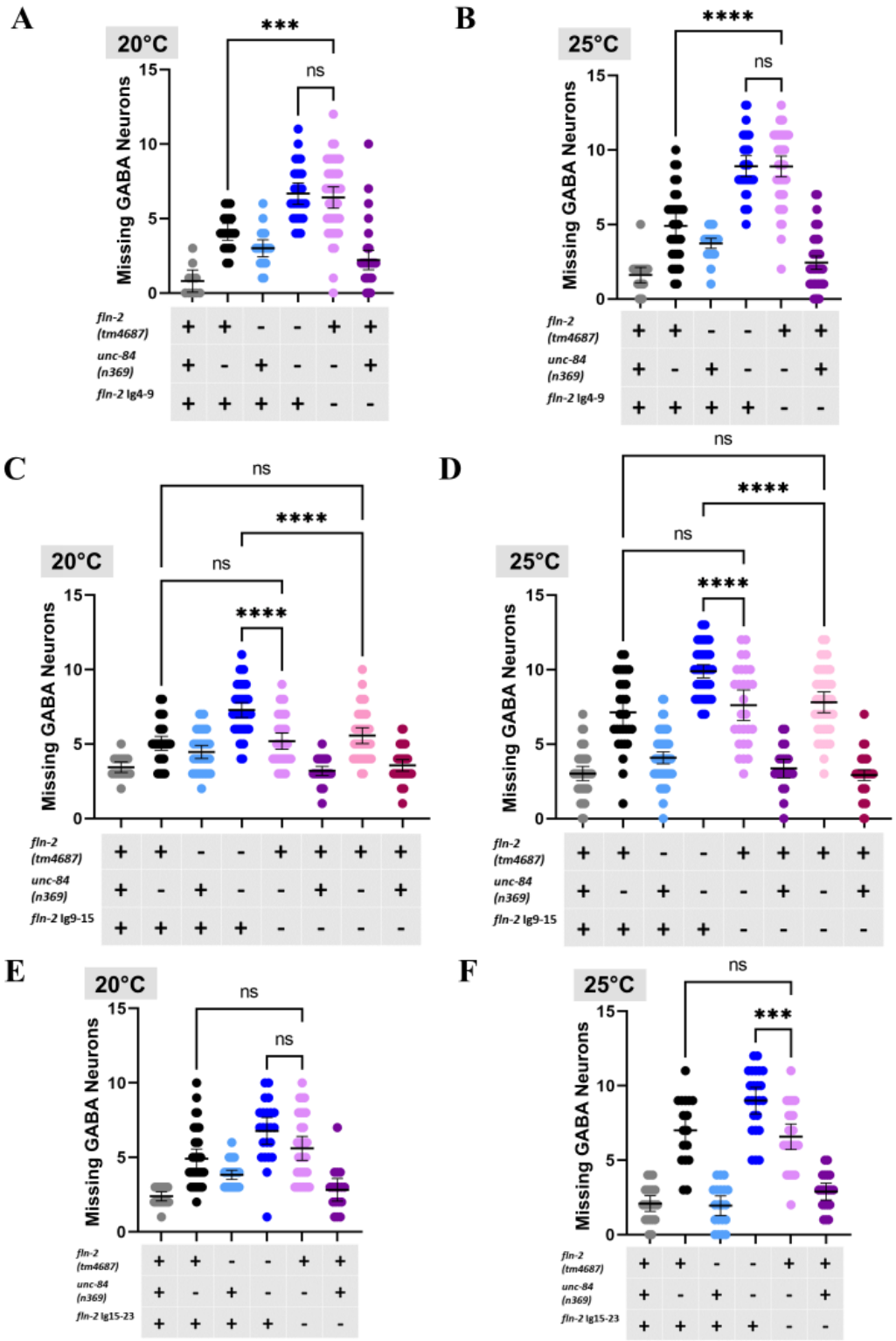

Supplemental Figure 2.2 FLN-2 Ig 4-8 are important in the restrictive temperatures, while Ig9-23 are not

The missing GABA neurons counts for the *fln-2* Ig4-9 *unc-84(n369)* double mutants, single mutants, and wild-type animals are shown at 20°C in **A)** and 25°C in **B)**. The missing GABA neurons counts for the *fln-2* Ig9-15 *unc-84(n369)* double mutants, single mutants, and wild-type animals are shown at 20°C in **C)** and 25°C in **D)**. The missing GABA neurons counts for the *fln-2* Ig15-23 *unc-84(n369)* double mutants, single mutants, and wild-type animals are shown at 20°C in **E)** and 25°C in **F)**. *** indicates p-value of 0.0003, **** indicates a p-value < 0.0001, all error bars are 95% confidence intervals and a one-way ANOVA test was done to generate p-values.

Table 2.1: List of worm strains used in this study

Strain	Genotype	Reference
N2	Bristol, wild-type	
FX4687	*fln-2(tm4687)*	(Barstead et al., 2012)
UD87	*unc-84(n369); oxIs12[unc-47::gfp, dpy-20(+)]; ycEx60[odr-1::rfp, WRM0617cH07]*	(Chang et al., 2013)
UD363	*fln-2(tm4687) unc-84(n369) ycEx202[odr-1::gfp; phlh-3::nls::tdTomato; phlh-3::vab-10-abd::mVenus]*	This study
UD368	*unc-84(n369) fln-2(tm4687); juIs76[unc-25::gfp] II*	This study
UD370	*fln-2(tm4687) juIs76[unc-25::gfp] II +/-*	This study
UD381	*ycIs11[odr-1::gfp; phlh-3::vab-10-abd::mVenus; phlh-3::nls::tdTomato]*	(Chang et al., 2013)
UD407	*unc-84(n369) ycIs11[odr-1::gfp; phlh-3::vab-10-abd::mVenus; phlh-3::nls::tdTomato]*	(Bone et al., 2016)
UD593	*ycSi1[phlh3::lifeact::mKate2 pCFJ150[unc-119(+)]II*	This study
UD614	*ycEx283[10ng/ul phlh3::nls::gfp::lacZ, 90ng/ul odr-1::gfp] ycSi1[phlh3::lifeact::mKate2 pCFJ150[unc-119(+)]II*	This study
UD727	*unc-84(n369); fln-2(tm4687) ycEx[unc-47::gfp] ycEx261[(5ng/ul WRM0625B05), (95ng/ul pGH8 (prab-3::mCherry))]*	This study
UD746	*unc-84(n369); oxIs12[unc-47::gfp, dpy-20(+)]; yc115[fln-2c(ΔIg9-15)]X, dpy-10(+)*	This study
UD747	*unc-84(n369); oxIs12[unc-47::gfp, dpy-20(+)];yc115[fln-2c(ΔIg9-15)]X, dpy-10(+)*	This study
UD749	*unc-84(n369); oxIs12[unc-47::gfp, dpy-20(+)];yc115[fln-2c(ΔIg9-15)]X, dpy-10(+)*	This study
UD759	*unc-84(n369); oxIs12[unc-47::gfp, dpy-20(+)] yc114[fln-2c(ΔIg4-9); dpy-10(+)*	This study
UD771	*yc117[spGFP11::fln-2c]X*	This study

UD774	*yc117[spGFP11::fln-2c ycEx265[2ng/ul pSL830, 98ng/ul odr-1::gfp]*	This study
UD799	*unc-84(n369); yc116[fln-2c(ΔIg15-23(-)]X; oxIs12[unc-47::gfp] +ycEx60[odr-1::rfp, unc-84(+)]*	This study
UD801	*unc-84(n369); yc116[fln-2c(ΔIg15-23(-)]X; oxIs12[unc-47::gfp] +ycEx60[odr-1::RFP, unc-84(+)]*	This study
UD807	*ycIs15[phlh3::nls::gfp::lacZ, odr-1::gfp phlh3::lifeact::mKate2 pCFJ150[unc-119(+)]II*	This study
UD847	*ycIs11[odr-1::gfp; phlh-3::vab-10-abd::mVenus; phlh-3::nls::tdTomato]; fln-2(tm4687)*	This study

Table 2.1 List of worm strains used in this study
This is a list of all worm strains used in our studies and their genotypes.

Table 2.2 CRISPR crRNA and ssODN Sequences

New allele	Strain	crRNA	ssODN repair template
[fln-2c(ΔIg4-9)]X	UD87	ATGGAGCATCGGGTACACGT	ACCGACGTGCACCCGATGTTCCATCTGCTTGCAATTACGACCCAGCCAAAATTAAAGTCGGAGCAATTCC
		GATCCAGCTAAGATTAAAGT	
[fln-2c(ΔIg9-15)]X	UD87	TGTCCAACCCTGGAAAGCGA	CCGCCAAAACTACCGTTTCCAAAATTCCATCACTCTTAGATCCATCAGCTGTGAGAGTTATTGGACTGAAAAATGCTCC
		AGCGTGGATTATACTAATAG	
[fln-2c(ΔIg15-23)]X	UD87	CTCAAGATACCTTCGCGGCG	AGCGCAAAATGCAAACAGTGATTGACCCACTTAATGTCGACACCGAGAAAGAACTCCCAAGACACGTTCG
		GATACACGTACTCCGCCGTC	
[spGFP::fln-2c]X	N2	agagccaggcgagcacagtg	tttcttgatttgcaggcgagcacagcgtcgatgtCATGAGAGATCACATGGTTCTTCATGAATATGTAAATGCAGCTGGAATTACAGGAGGTTCTGGCGGAATGCTAGCAGACCAACGTGTACCCGATGCTCCATT

Table 2.2 CRISPR crRNA and ssODN sequences

List of the CRISPR guides and repair templates used in this study.

Citation

Alzari, P.M. 1998. Domains, immunoglobulin-type. *Encycl. Immunol.* 43:1–9. doi:.1037//0033-2909.I26.1.78.

Barstead, R., G. Moulder, B. Cobb, S. Frazee, D. Henthorn, J. Holmes, D. Jerebie, M. Landsdale, J. Osborn, C. Pritchett, J. Robertson, J. Rummage, E. Stokes, M. Vishwanathan, S. Mitani, K. Gengyo-Ando, O. Funatsu, S. Hori, R. Imae, E. Kage-Nakadai, H. Kobuna, E. Machiyama, T. Motohashi, M. Otori, Y. Suehiro, S. Yoshina, D.G. Moerman, M. Edgley, R. Adair, B. Allan, V. Au, I. Chaudhry, R. Cheung, O. Dadivas, S. Eng, L. Fernando, A. Fisher, S. Flibotte, E. Gilchrist, A. Hay, P. Huang, R.W. Hunt, C. Kwitkowski, J. Lau, N. Lee, L. Liu, A. Lorch, C. Luck, J. Maydan, S. McKay, A. Miller, G. Mullen, C. Navaroli, S. Neil, R. Hunt-Newbury, M. Partridge, J. Perkins, A. Rankin, G. Raymant, N. Rezania, A. Rogula, B. Shen, G. Stegeman, A. Tardif, J. Taylor, M. Veiga, T. Wang, and R. Zapf. 2012. Large-scale screening for targeted knockouts in the caenorhabditis elegans genome. *G3 Genes, Genomes, Genet.* 2:1415–1425. doi:10.1534/g3.112.003830.

Barzilai, S., S.K. Yadav, S. Morrell, F. Roncato, E. Klein, L. Stoler-Barak, O. Golani, S.W. Feigelson, A. Zemel, S. Nourshargh, and R. Alon. 2017. Leukocytes Breach Endothelial Barriers by Insertion of Nuclear Lobes and Disassembly of Endothelial Actin Filaments. *Cell Rep.* 18:685–699. doi:10.1016/j.celrep.2016.12.076.

Berger, S., S. Spiri, A. deMello, and A. Hajnal. 2021. Microfluidic-based imaging of complete Caenorhabditis elegans larval development. *Dev.* 148. doi:10.1242/DEV.199674.

Bone, C., Y.-T. Chang, N.E. Cain, S.P. Murphy, and D.A. Starr. 2016. Nuclei migrate through constricted spaces using microtubule motors and actin networks in C. elegans hypodermal cells. *Development*. 143:4193–4202.

Bone, C.R., and D.A. Starr. 2016. Nuclear migration events throughout development. *J. Cell Sci.* 129:1951–1961. doi:doi:10.1242/jcs.179788.

Cabantous, S., T.C. Terwilliger, and G.S. Waldo. 2005. Protein tagging and detection with engineered self-assembling fragments of green fluorescent protein. *Nat. Biotechnol.* 23:102–107. doi:10.1038/nbt1044.

Chang, Y.-T., D. Dranow, J. Kuhn, M. Meyerzon, M. Ngo, D. Ratner, K. Warltier, and D.A. Starr. 2013. toca-1 Is in a Novel Pathway That Functions in Parallel with a SUN-KASH Nuclear Envelope Bridge to Move Nuclei in Caenorhabditis elegans. *Genetics*. 193:187–200.

DeMaso, C.R., I. Kovacevic, A. Uzun, and E.J. Cram. 2011. Structural and Functional Evaluation of C. elegans Filamins FLN-1 and FLN-2. *PLoS One*. 6:e22428. doi:10.1371/journal.pone.0022428.

Doonan, R., J. Hatzold, S. Raut, B. Conradt, and A. Alfonso. 2008. HLH-3 is a C. elegans Achaete/Scute protein required for differentiation of the hermaphrodite-specific motor neurons. *Mech. Dev.* 125:883–893. doi:10.1016/j.mod.2008.06.002.

Farboud, B., A.F. Severson, and B.J. Meyer. 2019. Strategies for Efficient Genome Editing Using CRISPR-Cas9. *Genetics*. 211:431–457. doi:10.1534/genetics.118.301775.

Fraser, A.G., R.S. Kamath, P. Zipperlen, M. Martinez-Campos, M. Sohrmann, and J. Ahringer. 2000. Functional genomic analysis of C. elegans chromosome I by systematic RNA interference. *Nature*. 408:325–330. doi:10.1038/35042517.

Fridolfsson, H.N., L.A. Herrera, J.N. Brandt, N.E. Cain, G.J. Hermann, and D.A. Starr. 2018.

Genetic Analysis of Nuclear Migration and Anchorage to Study LINC Complexes During Development of Caenorhabditis elegans. Humana Press, New York, NY. 163–180.

Frøkjær-Jensen, C., M.W. Davis, M. Ailion, and E.M. Jorgensen. 2012. Improved Mos1-mediated transgenesis in C. elegans. *Nat. Methods*. 9:117–118. doi:10.1038/nmeth.1865.

Frøkjær-Jensen, C., M.W. Davis, M. Sarov, J. Taylor, S. Flibotte, M. LaBella, A. Pozniakovsky, D.G. Moerman, and E.M. Jorgensen. 2014. Random and targeted transgene insertion in Caenorhabditis elegans using a modified Mos1 transposon. *Nat. Methods*. 11:529–534. doi:10.1038/nmeth.2889.

Frøkjær-Jensen, C., M. Wayne Davis, C.E. Hopkins, B.J. Newman, J.M. Thummel, S.P. Olesen, M. Grunnet, and E.M. Jorgensen. 2008. Single-copy insertion of transgenes in Caenorhabditis elegans. *Nat. Genet.* 40:1375–1383. doi:10.1038/ng.248.

Gay, O., B. Gilquin, F. Nakamura, Z.A. Jenkins, R. McCartney, D. Krakow, A. Deshiere, N. Assard, J.H. Hartwig, S.P. Robertsone, and J. Baudier. 2011. RefilinB (FAM101B) targets FilaminA to organize perinuclear actin networks and regulates nuclear shape. *Proc. Natl. Acad. Sci. U. S. A.* 108:11464–11469. doi:10.1073/pnas.1104211108.

Gimona, M., K. Djinovic-Carugo, W.J. Kranewitter, and S.J. Winder. 2002. Functional plasticity of CH domains. *FEBS Lett.* 513:98–106. doi:10.1016/S0014-5793(01)03240-9.

Gorlin, J.B., R. Yamin, S. Egan, M. Stewart, T.P. Stossel, D.J. Kwiatkowski, and J.H. Hartwig. 1990. Human endothelial actin-binding protein (ABP-280, nonmuscle filamin): A molecular leaf spring. *J. Cell Biol.* 111:1089–1105. doi:10.1083/jcb.111.3.1089.

Ho, J., V.A. Valdez, L. Ma, and D.A. Starr. 2018. Characterizing Dynein' s Role in P-cell Nuclear Migration using an Auxin-Induced Degradation System. 1:2016–2018.

Kamath, R.S., A.G. Fraser, Y. Dong, G. Poulin, R. Durbin, M. Gotta, A. Kanapin, N. Le Bot, S. Moreno, M. Sohrmann, D.P. Welchman, P. Zipperien, and J. Ahringer. 2003. Systematic functional analysis of the Caenorhabditis elegans genome using RNAi. *Nature*. 421:231–237. doi:10.1038/nature01278.

Kim, H.S., R. Murakami, S. Quintin, M. Mori, K. Ohkura, K.K. Tamai, M. Labouesse, H. Sakamoto, and K. Nishiwaki. 2011. VAB-10 spectraplakin acts in cell and nuclear migration in Caenorhabditis elegans. *Development*. 138:4013–4023. doi:10.1242/dev.059568.

Köppen, M., J.S. Simske, P.A. Sims, B.L. Firestein, D.H. Hall, A.D. Radice, C. Rongo, J.D. Hardin, S. Cell, L.F. Kimball, N. York, E. Street, N. York, and N. York. 2001. Cooperative regulation of AJM-1 controls junctional integrity in Caenorhabditis elegans epithelia articles. *Nat Cell Biol*. 3:983–991.

Kovacevic, I., and E.J. Cram. 2010. FLN-1/Filamin is Required for Maintenance of Actin and Exit of Fertilized Oocytes from the Spermatheca in C. elegans. *Dev. Biol.* 347:247–257. doi:10.1016/j.ydbio.2010.08.005.

Malone, C.J., W.D. Fixsen, H.R. Horvitz, and M. Han. 1999. UNC-84 localizes to the nuclear envelope and is required for nuclear migration and anchoring during C. elegans development. *Development*. 126:3171–3181.

McIntire S. L. Schuske K., Edwards R. H., Jorgensen E. M., R.R.J. 1997. Identification and characterization of the vesicular GABA transporter. *Nature*. 389:870–876.

Paix, A., A. Folkmann, D. Rasoloson, and G. Seydoux. 2015. High Efficiency, Homology-

Directed Genome Editing in Caenorhabditis elegans Using CRISPR-Cas9 Ribonucleoprotein Complexes. *Genetics*. 201:47–54. doi:10.1534/genetics.115.179382.

Paix, A., A. Folkmann, and G. Seydoux. 2017. Precision genome editing using CRISPR-Cas9 and linear repair templates in C. elegans. *Methods*. 121–122:86–93. doi:10.1016/j.ymeth.2017.03.023.

Riedl, J., A.H. Crevenna, K. Kessenbrock, J.H. Yu, D. Neukirchen, M. Bista, F. Bradke, D. Jenne, T.A. Holak, Z. Werb, M. Sixt, and R. Wedlich-Soldner. 2008. Lifeact: a versatile marker to visualize F-actin. *Nat. Methods*. 5:605. doi:10.1038/nmeth.1220.

Seyfried, T.N., and L.C. Huysentruyt. 2013. On the Origin of Cancer Metastasis. *Crit. Rev. Oncog.* 18:43–73.

Spear, P.C., and C.A. Erickson. 2012. Apical movement during interkinetic nuclear migration is a two-step process. *Dev. Biol.* 370:33–41. doi:10.1016/j.ydbio.2012.06.031.

Starr, D.A., G.J. Hermann, C.J. Malone, W. Fixsen, J.R. Priess, H.R. Horvitz, and M. Han. 2001. unc-83 encodes a novel component of the nuclear envelope and is essential for proper nuclear migration. *Development*. 128:5039–5050.

Stiernagle, T. 2006. Maintenance of C. elegans. *WormBook*. 1–11. doi:10.1895/wormbook.1.101.1.

Sulston, J.E., and H.R. Horvitz. 1977. Post-embryonic cell lineages of the nematode, Caenorhabditis elegans. *Dev. Biol.* 56:110–156. doi:https://doi.org/10.1016/0012-1606(77)90158-0.

Sulston, J.E., and H.R. Horvitz. 1981. Abnormal cell lineages in mutants of the nematode Caenorhabditis elegans. *Dev. Biol.* 82:41–55. doi:https://doi.org/10.1016/0012-1606(81)90427-9.

Thiam, H.-R., P. Vargas, N. Carpi, C.L. Crespo, M. Raab, E. Terriac, M.C. King, J. Jacobelli, A.S. Alberts, T. Stradal, A.-M. Lennon-Dumenil, and M. Piel. 2016. Perinuclear Arp2/3-driven actin polymerization enables nuclear deformation to facilitate cell migration through complex environments. *Nat. Commun.* 7:10997. doi:10.1038/ncomms10997http://www.nature.com/articles/ncomms10997#supplementary-information.

Tursun, B., L. Cochella, I. Carrera, and O. Hobert. 2009. A toolkit and robust pipeline for the generation of fosmid-based reporter genes in C. elegans. *PLoS One*. 4. doi:10.1371/journal.pone.0004625.

Chapter III: Future directions for elucidating FLN-2, CGEF-1, and Lamin's roles in the P-cell nuclear migration pathway

Specific Aims

Canonically, microtubule-based pathways have been the main mechanism by which P-cell nuclear migration through constricted spaces is regulated. In the microtubule-based pathway, the inner nuclear membrane protein UNC-84 (SUN protein) engages lamin in the nucleoskeleton and UNC-83 (KASH protein) in the perinuclear space. UNC-83 spans the perinuclear space to the outer nuclear membrane, where it recruits microtubule motors, such as cytoplasmic dynein and kinesin. This SUN-KASH bridge promotes nuclear migration along the microtubules through the constricted space (Bone et al., 2016; Ho et al., 2018; Meyerzon et al., 2009; Fridolfsson and Starr, 2010; Sosa et al., 2012; Starr, 2019). In the absence of this SUN-KASH bridge at 15°C, successful P-cell nuclear migration is on par with the wild-type. As such, there is normal development of the GABA neurons and vulva. At higher restrictive temperatures, there are significant P-cell nuclear migration failures, leading to *Egl* (egg-laying deficient) and *Unc* (uncoordinated) phenotypes. These *Egl* and *Unc* phenotypes result from the absence of a vulva and an improper number of GABA neurons (Starr et al., 2001; Malone et al., 1999; Sulston and Horvitz, 1981).

Our lab performed a forward genetics screen (Chang et al., 2013) and found two putative actin players, CGEF-1 and FLN-2. CGEF-1 is predicted to be a Cdc42 guanine exchange factor which activate Cdc42 by cycling Cdc42 from an off GDP-bound state to an on GTP-bound state (Chan and Nance, 2013; Etienne-Manneville and Hall, 2002; Etienne-Manneville, 2004). FLN-2, the focus of this thesis, is predicted to be a divergent filamin. Filamins canonically act to crosslink and bundle actin filaments (Nakamura et al., 2011), but the molecular mechanisms of FLN-2 in P-cell nuclear migration is unknown. We have also been interested in the role of lamins, an intermediate filament, forming the nucleoskeleton and involved in nuclear stiffness. Although filamin's defined role is in interacting with actin, our data show that FLN-2C lacks the N-terminal actin binding domain and does not appear to colocalize

with actin either *in vivo* nor in U2OS cells. Therefore I hypothesize that FLN-2C is not directly binding to actin but is further upstream of the pathway. Filamin dimers canonically respond to mechanical forces, so my working model is that FLN-2 serves as a force sensor and activates a pathway upstream of the formation of branched actin networks. CGEF-1 in the context of P-cell nuclear migration is predicted to activate Cdc42, the subsequent WAVE/WASp machinery, and Arp2/3, building branched actin networks to deform the nuclear as it migrates. Lamins make up the integrity of the nucleoskeleton and it has been predicted that there must be a balance of lamin (Harada et al., 2014; Swift et al., 2013), to ensure that the nucleus is neither too firm nor too soft, to successfully migrate. I hypothesize that these three proteins are acting in three different pathways to mediate nuclear migration.

To test this hypothesis, I am interested in the following aims: **1)** identifying other players in LINC-independent nuclear migration pathways **2)** determining which specific FLN-2c domains are required for P-cell nuclear migration, **3)** filming P-cell nuclear migration in wildtype and mutant animals happening in real time to measure kinetics of normal and *fln-2* mutants, **4)** conducting correlative light electron microscopy on a *C. elegans* L1 larvae in mid migration to measure the dimensions of the migration nucleus and the constriction. **5)** determining FLN-2's role as a force sensor with AFM and its effect on actin localization **6)** determining whether lamin and FLN-2 are in the same pathway with genetic tools **7)** determining how FLN-2 and CGEF-1 fit into P-cell nuclear migration and **8)** determining why and how micronuclei are formed. Understanding how these three very different proteins mediate nuclear migration through constricted spaces can shed some light on the mechanisms which may be implicated in cancer metastasis (Thiam et al., 2016), X-linked periventricular heterotopia (Ekşioğlu et al., 1996), and laminopathies (Harr et al., 2020; Starr, 2012).

3.1 Identifying other players in LINC-independent nuclear migration pathways

P-cell nuclear migration is canonically supported by the microtubule-based LINC complex-mediated pathway. However, previous literature has suggested the presence of alternative pathways acting at 15°C (Sulston and Horvitz, 1981). To explore these alternative pathways, I performed forward genetic screens with EMS (ethyl methanesulfonate) to uncover enhancers of the nuclear migration defect of *unc-84 (emu)*. At the beginning of my graduate career, I conducted several *emu* screens and found one potential *emu*. In this particular screen, I looked through a total of 1600 genomes, following the protocol I described in the introduction chapter (**Fig 1.4)**. We dubbed this allele *yc47*, finding that this *emu; unc-84(n369)* double mutant was missing an average of ~5.8 GABA neurons at the permissive temperature of 15°C (**Fig 3.1**). Subsequently, we sent this strain out for whole genome sequencing. My colleague, Xiangyi Ding, ran this *emu*, along with 8 other *emu* strains we found in previous screens (Chang et al., 2013) through a bioinformatics pipeline. She compared their respective genomes and found that CGEF-1 was one of the genes that was not found in all of these strains.

3.2 Determining which specific FLN-2c Ig-repeat is responsible for P-cell nuclear migration

My data in figure 2.1 shows that the shorter isoform, *fln-2c*, is sufficient for P-cell nuclear migration. Knocking out regions specific to larger isoforms does not result in a nuclear migration defect, as the *ot611* allele was identified in our starting strain and did not exhibit a nuclear migration defect (**Fig 2.1**). *fln-2c* lacks the N-terminal actin binding domain that canonical filamins possess (DeMaso et al., 2011). *fln-2c* consists of 20 immunoglobulin (Ig)-like repeats which are thought to facilitate protein-protein interactions. In other filamins, the C-terminal Ig-repeat acts as a dimerization/ self-association domain (Pudas et al., 2005; Fucini et al., 1997). Filamins also consist of two separate rods, made up of Ig-like repeats; the first rod binds to actin, while the second rod associates with partner proteins (Nakamura et al., 2011, 2007; Feng

et al., 2006). How each of these 20 Ig-like repeats, that make up *fln-2c*, functions is not yet known. Given that mammalian filamins interact directly with actin, I was interested in determining whether any FLN-2 Ig-repeats may bind to actin, and which repeats are important for P-cell nuclear migration.

I was able to narrow down the Ig-repeat of interest to Ig4-8 (**Fig 2.3**), I made attempts to target Ig4-6 and 6-8 but was unsuccessful. Further, when Ig4-8 was expressed in mammalian tissue culture, they did not appear to colocalize with actin (**Fig 2.5A**). It would be interesting to further divide the Ig-repeats into the two rod regions and perform a yeast two hybrid on these separate rods to determine what they may interact with and if these binding partners would be integral to P-cell nuclear migration.

3.3 Filming P-cell nuclear migration in wildtype and mutant animals happening in real time to measure kinetics

Understanding the rate at which nuclear migration and rupture occurs in wildtype and mutant animals would allow us to further probe the underlying mechanisms that support P-cell nuclear migration. We have long hypothesized that the P cells can migrate at the permissive temperature in the absence of the SUN-KASH bridge (Sulston and Horvitz, 1981), because migration occurs much more slowly at 15°C than at 25°C. Another possibility is that the microtubule pathway may be more dynamic or stable at 15°C than the actin pathway. To film this event occurring, we could tag the cytoskeletal components to better understand how they support nuclear migration and their dynamics.

We have attempted this feat through the 3i spinning disc confocal, the Zeiss Airyscan LSM, and the 3i lattice light sheet microscope but all attempts failed. Using the 3i spinning disc confocal and the Zeiss Airyscan LSM, we followed established methods in the lab (Fridolfsson et al., 2018) using 2% agarose pads, and 1uM tetramizole to paralyze L1 larvae that were in

varying stages of P-cell nuclear migration (pre-, mid-, and post-). In both cases, the P cells would fail to migrate even after extended imaging on the microscope. We theorized that the pressure from the coverslip, the paralytic, the laser intensity, or a combination of these may be too stressful for the worms to successfully develop. With the 3i lattice light sheet microscope, we were able to film worms for extended amounts of time (up to 12 hours) without bleaching out the fluorescent signal, but the worms failed to develop. We prepared these slides with PEGDA (Burnett et al., 2018), which allow the worms to develop, but any amount of paralytic would halt development.

We attempted to use the Newormics vivoChip, a microfluidic device which would use pressure to keep worms still and would not need paralytic to immobilize them. Unfortunately, this device did not allow us to feed the animals and so they failed to develop. We made these attempts on the 3i Spinning Disc Confocal. We have had some success on the Zeiss LSM Airyscan with a microfluidic device developed by our collaborators in Switzerland (Berger et al., 2021). This device is similar to the Newormics vivoChip, but allows the cycling of bacteria to keep the worms fed. Our collaborator has been able to film animals from the time they are embryos until they become adult animals. We have been able to film P-cell nuclear migration and division. With this new microfluidic device, we could express our *fln-2::GFP* in a strain with fluorescently tagged actin and nuclei to explore how FLN-2 may interact with actin and nuclei during migration. We could determine what is happening in the presence of FLN-2 and the absence, and how this may affect the kinetics of nuclear migration at the permissive and restrictive temperatures.

3.4 Conducting correlative light electron microscopy on a *C. elegans* embryo in mid migration to measure the dimensions of the migration nucleus and the constriction

We have long relied on electron micrographs of adult *Caenorhabditis elegans* to inform estimates on the dimensions of the nucleus and constriction (Rostaing et al., 2004). While this may give us a relative estimate of their sizes, this is not as good as the real thing. I made several attempts to conduct this experiment with our collaborators at the UC Berkeley EM core (Danielle Jorgens). In our first attempt, we were not able to successfully high pressure freeze worms. In our second attempt, we found that the *nls::tdTomato* signal was not preserved, though the *vab-10::mVenus* signal was preserved (**Fig 3.2**). Given that the green signal was preserved but the red signal was not, I decided to make a *lifeact::mKate2; nls::lacZ::GFP* (strain UD 614) worm so that we could measure the dimensions of the nucleus during nuclear migration. I successfully made the strain, with help from our undergraduate, Vivian Nguyen, with integrating this strain (UD 810). However, after a lot of work, I decided this high-risk project was taking up too much time and I focused on the other two aims.

If there is a future Starr lab member who wants to undertake this endeavor, I would advise you to remake the *lifeact::mKate2*; *nls::lacZ::GFP* strain so that the nls signal is not leaky. Though, this would require you to integrate the strain. To do this, it requires usage of the Cesium core. You can ask JoAnne Engebrecht for help on finding the cesium core. It also requires a commitment to screening for the successful integration event. I would advise recruiting an undergraduate to help with this project.

Further, if you could get this to work with the UC Davis EM core instead of the UC Berkeley EM core, it would make it less of a hassle to get all your worms down to UC Berkeley along with the Leica fluorescent dissecting microscope. Though you should get in contact with

Danielle Jorgens because she may remember how we were able to successfully get worms high pressure frozen and imaged on the TEM. This will save you some steps.

3.5 Determining FLN-2's role as a force sensor with AFM and its effect on actin localization

Canonical filamins have been implicated as force sensors that directly mediate actin. Given that FLN-2 does not appear to colocalize with actin *in vivo* and in mammalian cells (**Fig 2.5a**), the next step would be to determine if it even fulfills the role of a force sensor. The Mullins lab has previously reconstituted *in vitro* branched actin networks with purified actin, profilin, Arp2/3, capping protein, and nucleation promoting factor, and used AFM (atomic force microscopy) to determine the effect of varying forces and starting material on molecular composition (Bieling et al., 2016). I would be interested in determining how varying forces would affect FLN-2 and subsequently branched actin assembly and density. The Cabreiro lab has successfully used AFM to push on *C. elegans* cuticle and determine biomarkers in aging animals (Essmann et al., 2020).

One way to approach this would be to use AFM on my FLN-2:spGFP worm, simultaneously filming the event with a fluorescence microscope to determine if varying forces would affect actin density. I would push on the nucleus determine if applying varying forces would affect FLN-2 and actin localization. This would elucidate whether FLN-2 interacts with actin downstream and if FLN-2 is associating with the nucleus and acting as a force sensor. If FLN-2 expression increases in response to applied forces, this may implicate its role as a mechanosensor. If actin localization changes, this may implicate actin's role in nuclear migration through constricted spaces. There are AFMs on the UC Davis campus which we could use. Alternatively, Dyche Mullins and Dan Fletcher, just down the road from UC Davis could be potential collaborators.

3.6 Determining whether lamin and FLN-2 are in the same pathway with genetic tools

Nuclear deformation is often the rate limiting step for cellular migration through constricted spaces. The ability of a nucleus to flatten and squeeze through small interstitial spaces is determined by its lamin composition. Lower levels of lamin leads to less rigid nuclei, which allows for more efficient nuclear migration (Swift et al., 2013; Wiesel et al., 2007). Lamin is needed to stabilize the nuclear envelope and its absence increases the risk of nuclear rupture (Denais et al., 2016). Given this link to nuclear rupture, I would be interested in determining if FLN-2 and LMN-1 act in the same genetic pathway. *In vitro* studies have shown that cellular migration increases nuclear stress and a deformable nuclear envelope and DNA damage repair are essential for cell survival (Denais et al., 2016; Raab et al., 2016). Lamin has also been implicated in chromosome movement so that homologous chromosomes can correctly segregate during meiosis. This movement occurs when there is a reduction in lamin association with the nuclear rim. This process occurs when lamin is phosphorylated by the kinases CHK-2 and PLK-2 (Link et al., 2018; Velez-aguilera et al., 2020). We hypothesized that this phosphorylation and subsequent disassociation of lamin with the nuclear envelope will result in a more pliable nucleus. If too much lamin has been phosphorylated, the nucleus may be unable to migrate.

Here, we explore the role of phosphorylation in nuclear stiffness. Our collaborators in the Jantsch lab made several serine to alanine mutations in *lmn-1* with CRISPR. I then crossed these mutant strains into our *unc-84(n369)* mutant worms to determine if lamin phosphorylation mutations would affect P-cell nuclear migration. While mutating S32, 403, and 470 to alanine resulted in a significant GABA neuron loss in an *unc-84(n369)* background at 25°C, it did not result in a significant loss at the permissive temperature of 15°C (**Fig 3.3).** However, mutating S21, 22, 24, 32, 397, 403, and 405 to alanine produced a significant loss at the permissive

temperature of 15°C (**Fig 3.3**). This indicates that being unable to phosphorylate these 7 serine residues of *lmn-1* affects the ability of the nuclei to properly migrate through the narrow constriction. The Jantsch lab has shown that LMN-1 is phosphorylated during *C. elegans* meiosis, which results in a more soluble lamina. This then triggers chromatin reorganization, and the inability to phosphorylate lamin will result in a stiff nucleus and subsequently delayed meiosis, unpaired or interlocked chromosomes, and slowed chromosome movement (Link et al., 2018). Thus, this P-cell nuclear migration defect may be due to a stiffer nucleus from the inability to phosphorylate these lamin in the *lmn-1(S21, 22, 24, 32, 397, 403, 405a)*, while the *lmn-1(S32, 403, 470)* mutant has a lesser effect due to being able to phosphorylate more sites.

Given LMN-1's role in P-cell nuclear migration and rupture, the next logical step would be to create a *fln-2(tm4687) unc-84(n369); lmn-1(S21, 22, 24, 32, 397, 403, 405a)* triple mutant and determining via the GABA neuron assay whether FLN-2 and LMN-1 are in the same genetic pathway.

3.7 Determining how FLN-2 and CGEF-1 fit into P-cell nuclear migration

Given that neither the *cgef-1* nor the *fln-2* double mutants resulted in a complete loss of P-cell derived GABA neurons (Chapter 2, Ho et al, personal communication), I wanted to test if *fln-2* and *cgef-1* were acting in the same pathway to mediate P-cell nuclear migration through constricted spaces. To test my hypothesis, I used RNAi to create a *fln-2(RNAi) cgef-1 (gk261) unc-84(n369)* triple mutant and determine if these two *emus* (enhancers of the nuclear migration defect of *unc-84*) were acting in the same pathway or separate pathways. CGEF-1 is predicted to be a CDC42 guanine exchange factor, stimulating the cycling of GDP-bound inactive-CDC42 to the GTP-bound active-CDC42 (Chan and Nance, 2013; Etienne-Manneville and Hall, 2002; Etienne-Manneville, 2004). FLN-2 is a divergent filamin, which canonically act as actin crosslinkers and bundlers (Nakamura et al., 2011). CGEF-1 (Kumfer et al., 2010; Chan and Nance, 2013) and filamins are putative actin players (Stossel et al., 2001; Nakamura et al.,

2011), so we were particularly interested in the result. We used RNAi given that all three genes were located on the X chromosome and a cross would be difficult. This data should be examined with the caveat that RNAi does not result in a complete knockout. However, the *fln-2(RNAI) unc-84(n369)* double mutant was able to recapitulate the *fln-2(tm4687) unc-84(n369)* double mutant phenotype.

I found that *fln-2* RNAi significantly enhanced the nuclear migration defect of the *unc-84; cgef-1* double mutant (**Fig 3.4**). These data are consistent with a model where *fln-2* and *cgef-1* were acting in separate pathways. It is not yet known how these two *emus* may function to promote P-cell nuclear migration. *fln-2* seems to help promote complete and stable nuclear migration (Chapter 2), we have not yet tagged our *cgef-1 unc-84* double mutant with a nuclear and actin marker to determine whether nuclear rupture occurs.

3.8 Determining why and how micronuclei are formed

Micronuclei have often been associated with nuclear rupture events (Hatch et al., 2013; Kwon et al., 2020). This may be due to the mechanical stress being exerted on the nucleus as it migrates through tight constrictions. *Caenorhabditis elegans* P cells must migrate from the lateral part of the hypodermis to the ventral part of the worm, through a tight constriction about 5% the diameter of the nucleus. In the ventral part of the hypodermis, these cells eventually divide and develop into the precursors to the GABA neurons and vulva. This process is supported by a microtubule-based pathway, involving the inner nuclear membrane protein, UNC-84, which recruits the outer nuclear membrane protein, UNC-83. UNC-83 recruits microtubule motors which facilitates migration through this small constriction (Starr, 2019; Ho et al., 2018; Bone et al., 2016; Sulston and Horvitz, 1981; Malone et al., 1999; Fridolfsson and Starr, 2010). In the past, we have wondered how these nuclei can migrate through such a small space without any sort of damage.

We have observed that micronuclei form before and during migration in our *unc-84* mutants, suggesting that these nuclei are not migrating without consequences, given that they are not as prevalent in our wild-type animals (**Fig 3.5a-b**). However, they are not present once migration has completed, and the disappearance of these micronuclei coincides with the occurrence of nuclear rupture (Section 2.4). In early migration, the number of micronuclei in *unc-84(n369)* single and *fln-2(tm4687) unc-84(n369)* double mutants were both significantly more than the wild-type, but the double mutant did not develop more micronuclei than the *unc-84(n369)* single mutant. This suggests that *fln-2(tm4687)* may not be involved in a pathway that prevents the formation of micronuclei. Micronuclei formation has been associated with chromosome mis-segregation during mitosis (Ungricht and Kutay, 2017), reduced nuclear function, and DNA damage (Hatch et al., 2013). Previously, it was unknown what happens during failed P-cell nuclear migration in *unc-84(n369)* mutants. One possible model I would like to propose is that the greater number of micronuclei in early migration are due to the initial migration attempts of the *unc-84* mutant P-cell nuclei. As a result of the mechanical stress from the constriction, they will then continue to develop micronuclei and eventually rupture. It would be interesting to film the formation of these micronuclei in real time to determine how they develop and what may cause them. Further, we could follow cells which have extensive formation of micronuclei and examine how and whether their vulva and GABA neurons develop successfully.

Summary

My current working model is that UNC-84, FLN-2, LMN-1, and CGEF-1 act in separate P-cell nuclear migration pathways. With UNC-84 taking the charge in the microtubule-based pathway, by recruiting UNC-83, and subsequently the microtubule motors, kinesin and dynein to facilitate migration along the microtubule tracks from the lateral to ventral part of the P cell. CGEF-1 is proposed to act as a CDC-42 guanine exchange factor (Etienne-Manneville, 2004;

Etienne-Manneville and Hall, 2002; Chan and Nance, 2013), activating the WAVE/WASp, ARP2/3 machinery to produce branched actin, which push on the nuclear envelope to deform it during migration. LMN-1 is phosphorylated to allow for proper nuclear pliability, but a limited number of sites must be phosphorylated to prevent the nucleus from being too 'soft' to migrate through the constriction. FLN-2 appears to help UNC-84 prevent nuclear rupture and micronuclei, and on its own, the mutant causes a significant number of P-cell nuclear migration defective events. FLN-2 is not currently shown to colocalize with actin either in mammalian cells nor *in vivo*, it would be pertinent to further characterize what is upstream and downstream of FLN-2.

My colleague, Ellen Gregory is already looking at the effect of *lmn-1* mutations on the formation of micronuclei, and my colleague Hongyan Hao has seen the formation of micronuclei in a different cell type in the *unc-83/ unc-84* pathway. In the future this and other work in the Starr lab will identify all of the different players which support P-cell nuclear migration, and how these different pathways intersect to contribute to migration, rupture, and the development of micronuclei.

Figures

Figure 3.1 The *yc47* allele is an enhancer of the nuclear migration defect of *unc-84* and the screen has been saturated

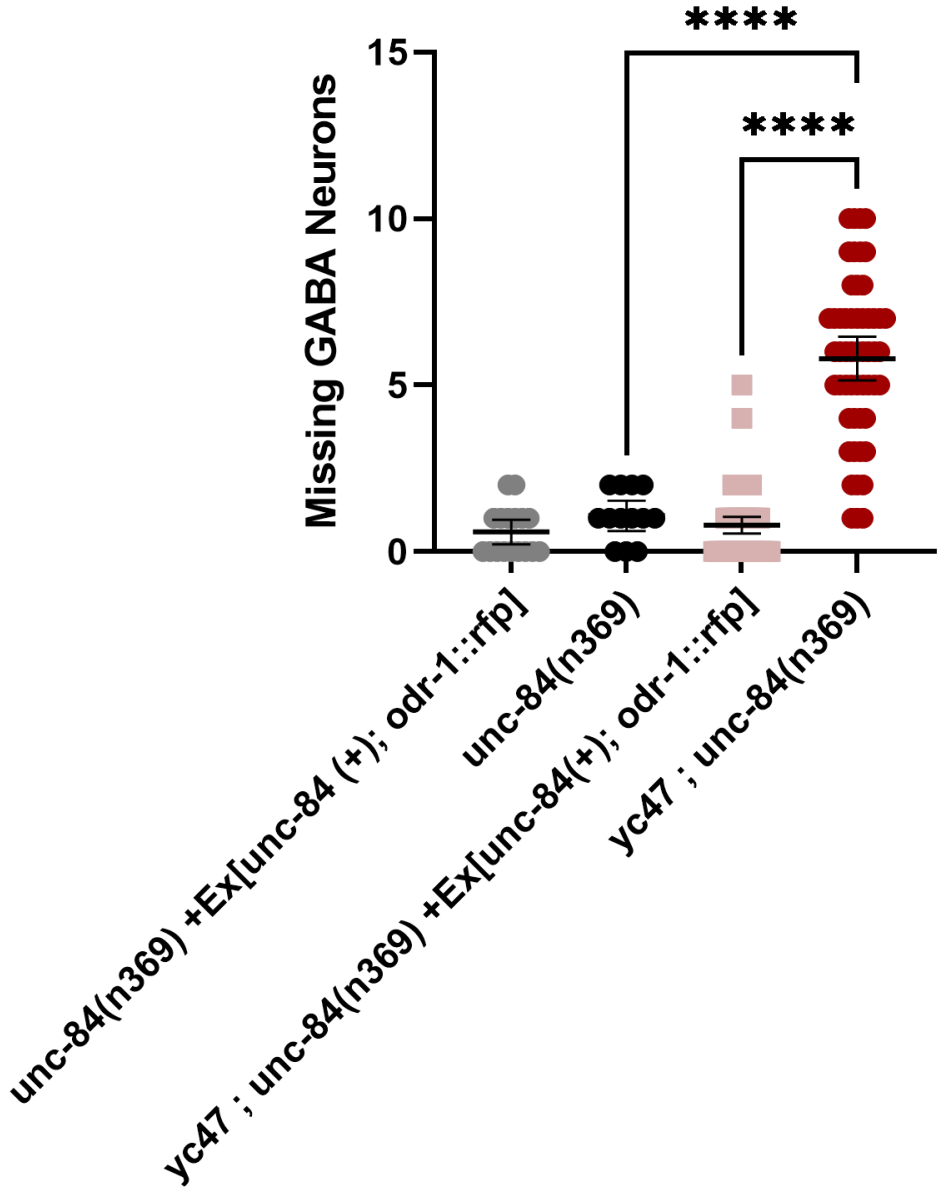

Figure 3.1 The *yc47* allele is an enhancer of the nuclear migration defect of *unc-84* and the screen has been saturated

This graph indicates the number of failed P-cell nuclear migration events in the wild-type and *unc-84(n369)* and *yc47* single and double mutants. All error bars are 95% CI, and **** indicates a P-value of < 0.0001. These experiments were conducted at 15°C

Figure 3.2 Fluorescence microscopy image of a HPF slice of the actin surrounding three different P-cells

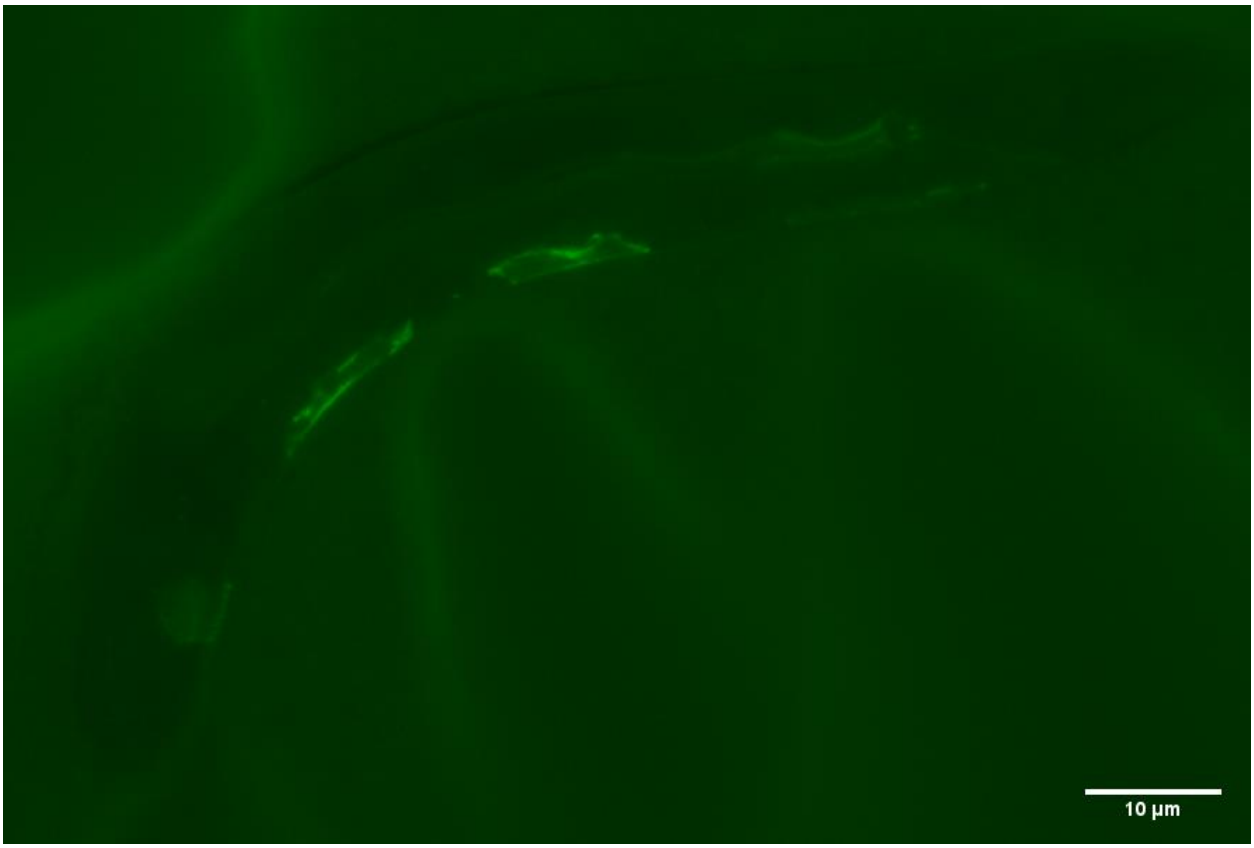

Figure 3.2 Fluorescence microscopy image of a HPF slice of the actin surrounding three different P-cells

This is an image of a *C. elegans* L1 larva that has been tagged with *vab-10::mVenus* and high pressure frozen. This image is a representation of a small slice of the HPF block. The scale bar indicates 10 microns. This image was taken on a wide-field epifluorescent Leica DM6000 wide-field epifluorescent Leica DM6000 microscope with a 63× Plan Apo 1.40 NA objective, a Leica DC350 FX camera, and Leica LAS AF software.

Figure 3.3 Phosphorylation of Lamin limits P-cell nuclear migration

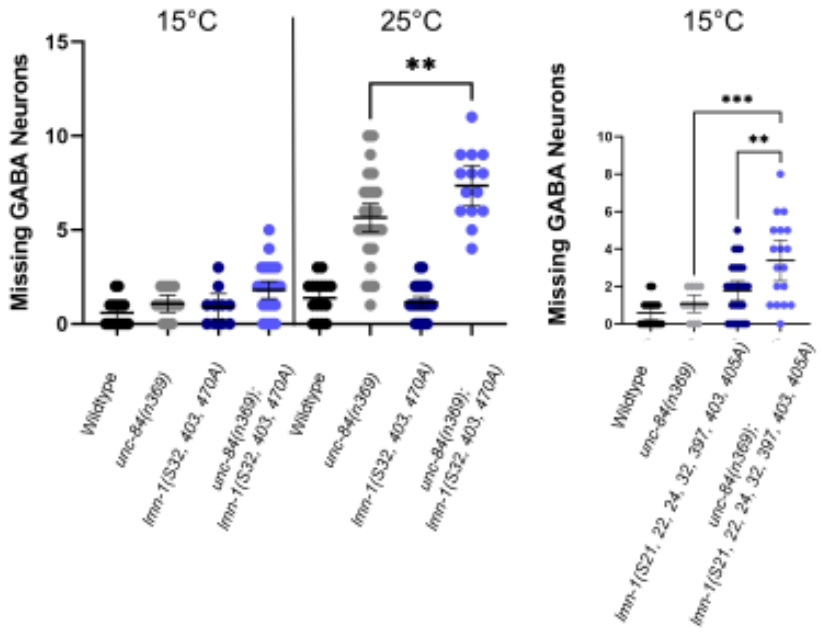

Figure 3.3 Phosphorylation of Lamin limits P-cell nuclear migration

This graph indicates the number of failed P-cell nuclear migration events in the wild-type and double mutants of *unc-84(n369)* and the lamin phosphorylation mutants (*lmn-1(S32, 403, 470A)* and *lmn-1(S21, 22, 24, 32, 397, 403, 405A*). All error bars are 95% CI, and **** indicates a P-value of < 0.0001. These experiments were conducted at 15°C

Figure 3.4 FLN-2 and CGEF-1 do not function in the same pathway

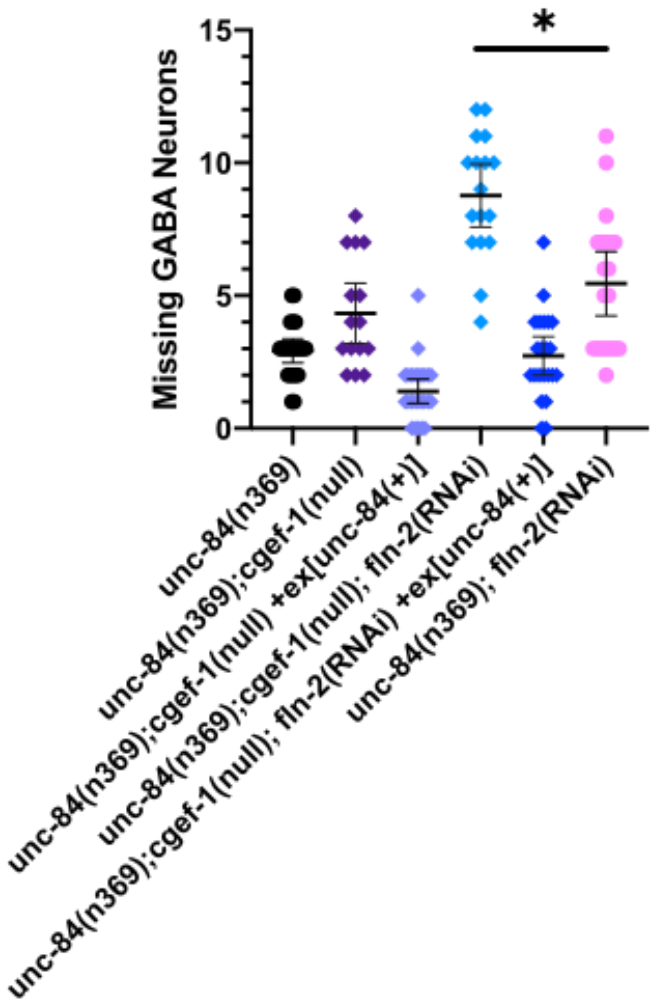

Figure 3.4 FLN-2 and CGEF-1 do not function in the same pathway

This graph indicates the number of failed P-cell nuclear migration events in the wild-type, single mutants (*unc-84(n369)* and *cgef-1(gk261)*), double mutants (*fln-2(RNAi) unc-84(n369)* and *unc-84(n369) cgef-1(gk261)*), and the triple mutant (*fln-2(RNAi) unc-84(n369) cgef-1(gk261)*). All error bars are 95% CI, and **** indicates a P-value of < 0.0001. These experiments were conducted at 15°C .

Figure 3.5 *unc-84* mutants form a significant number of micronuclei during nuclear migration through constricted spaces

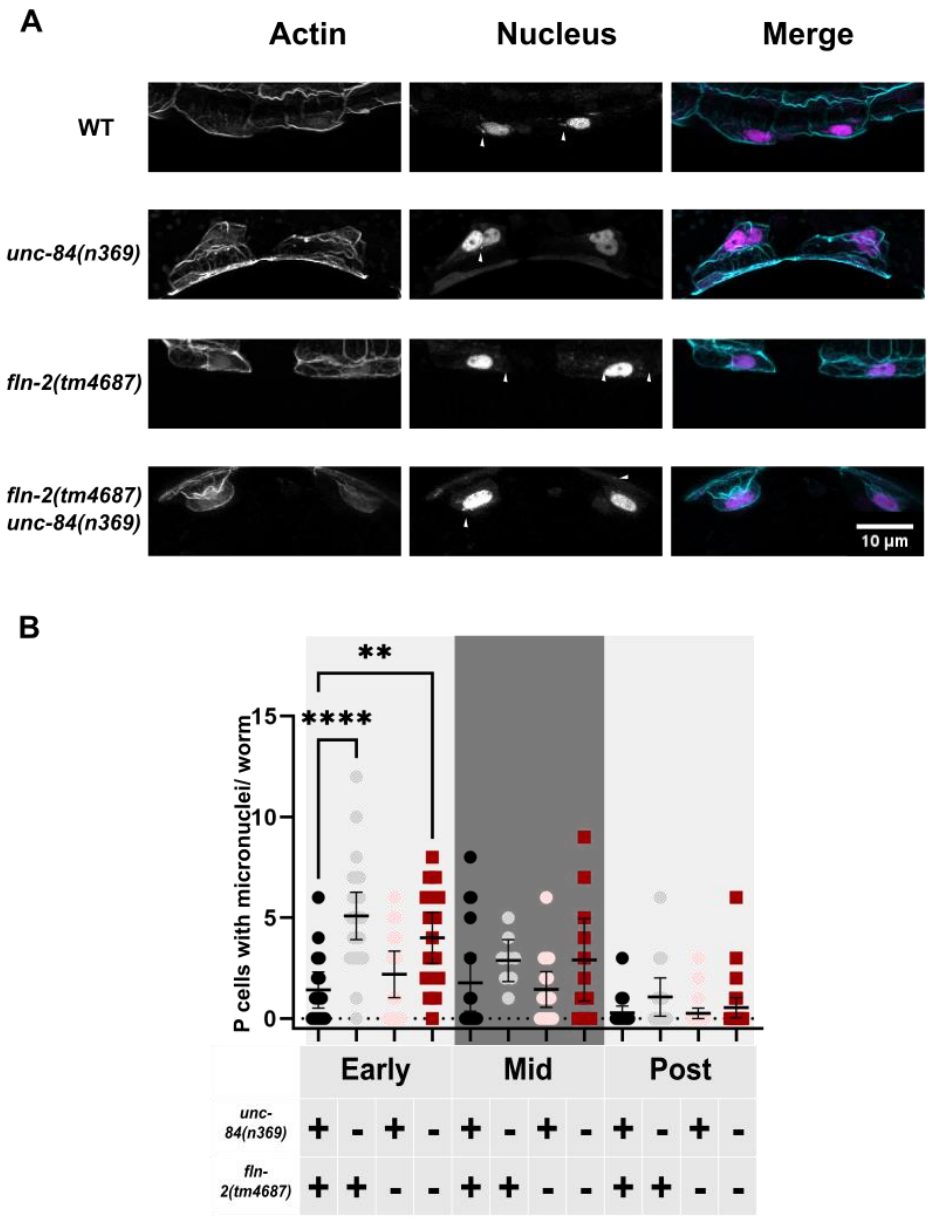

Figure 3.5 *unc-84* mutants form a significant number of micronuclei during nuclear migration through constricted spaces

A) These are representative images of wild-type, *fln-2(tm4687)*, *unc-84(n369)*, and the *fln-2(tm4687) unc-84(n369)* double mutant in early P-cell nuclear migration. With the actin tagged with mVenus, and the nuclei tagged with TdTomato. **B)** This is a graph indicating the number of P-cells with micronuclei per worm of wild-type, *fln-2(tm4687)*, *unc-84(n369)*, and the *fln-2(tm4687) unc-84(n369)* double mutant. All error bars are 95% CI, ** indicates P-value of <0.001, **** indicates a P-value of < 0.0001.

Table 3.1 Strains used in these studies

Strain Name	Genotype	Reference
UD87	*unc-84(n369);OxIs12[unc-47:gfp];ycEx60[odr-1:rfp, unc-84(+)]*	(Chang et al., 2013)
UD285	*yc3; unc-84(n369); OxIs12 X; ycEx60*	(Chang et al., 2013)
UD363	*fln-2(tm4687) unc-84(n369) ycEx202[odr-1::gfp; phlh-3::nls::tdtomato; phlh-3::vab-10-abd::mVenus]*	This study
UD381	*ycIs11[odr-1::gfp; phlh-3::vab-10-abd::mVenus; phlh-3::nls::tdTomato]*	(Chang et al., 2013)
UD407	*unc-84(n369) ycIs11[odr-1::gfp; phlh-3::vab-10-abd::venus; phlh-3::nls::tdTomato]*	This study
UD556	*lmn-1(tm1502)I;jfSi76[lmn-1(S32,403,470A)cb-unc-119(+)]II unc-84(n369)x;OxIs12[unc-47: GFP, dpy-20(+)]ycEx60[odr-1:RFP,unc-84(+)]*	This study
UD557	*unc-84(n369);OxIs12[unc-47:gfp];ycEx60[odr-1:rfp, unc-84(+)]; yc47*	This study
UD624	*lmn-1(jf136[S21, 22, 24, 32, 397, 398, 403, 405A]) unc-84(n369); oxIs12[unc-47::GFP]ycEx60[odr-1::RFP unc-84(+)]*	This study
UD810	*ycIS15[[phlhl3::nls::gfp::lacz; odr-1::GFP] [phlh-3::lifeact::mkate2]]II*	This study
UD847	*ycIs11[odr-1::gfp; phlh-3::vab-10-abd::venus; phlh-3::nls::tdTomato]; FLN-2(tm4687)*	This study

Table 3.1 Strains used in these studies

These are the strain names and their corresponding genotypes used in this chapter.

Citations

Bieling, P., T.-D. De Li, J. Weichsel, R. McGorty, P. Jreij, B. Huang, D.A.A. Fletcher, and R.D.D. Mullins. 2016. Force Feedback Controls Motor Activity and Mechanical Properties of Self-Assembling Branched Actin Networks. *Cell*. 164:115–127. doi:10.1016/j.cell.2015.11.057.

Bone, C., Y.-T. Chang, N.E. Cain, S.P. Murphy, and D.A. Starr. 2016. Nuclei migrate through constricted spaces using microtubule motors and actin networks in C. elegans hypodermal cells. *Development*. 143:4193–4202.

Chan, E., and J. Nance. 2013. Mechanisms of CDC-42 activation during contact-induced cell polarization. *J. Cell Sci.* 126:1692–1702. doi:10.1242/jcs.124594.

Chang, Y.-T., D. Dranow, J. Kuhn, M. Meyerzon, M. Ngo, D. Ratner, K. Warltier, and D.A. Starr. 2013. toca-1 Is in a Novel Pathway That Functions in Parallel with a SUN-KASH Nuclear Envelope Bridge to Move Nuclei in Caenorhabditis elegans. *Genetics*. 193:187–200.

Denais, C.., R.M. Gilbert, P. Isermann, A.L. McGregor, M. te Lindert, B. Weigelin, P.M. Davidson, P. Friedl, K. Wolf, and J. Lammerding. 2016. Nuclear envelope rupture and repair during cancer cell migration. *Science (80-.).* 352:353–358.

Ekşioğlu, Y.Z., I.E. Scheffer, P. Cardenas, J. Knoll, F. DiMario, G. Ramsby, M. Berg, K. Kamuro, S.F. Berkovic, G.M. Duyk, J. Parisi, P.R. Huttenlocher, and C.A. Walsh. 1996. Periventricular heterotopia: An X-linked dominant epilepsy locus causing aberrant cerebral cortical development. *Neuron*. 16:77–87. doi:10.1016/S0896-6273(00)80025-2.

Essmann, C.L., D. Martinez-Martinez, R. Pryor, K. Leung, K.B. Krishnan, P.P. Lui, N.D.E. Greene, A.E.X. Brown, V.M. Pawar, M.A. Srinivasan, and F. Cabreiro. 2020. Mechanical properties measured by atomic force microscopy define health biomarkers in ageing C. elegans. *Nat. Commun.* 11:1–16. doi:10.1038/s41467-020-14785-0.

Etienne-Manneville, S. 2004. Cdc42 - the centre of polarity. *J. Cell Sci.* 117:1291–1300. doi:10.1242/jcs.01115.

Etienne-Manneville, S., and A. Hall. 2002. Rho GTPases in cancer cell biology. *Nature*. 420:629–635. doi:10.1016/j.febslet.2008.04.039.

Fridolfsson, H.N., and D.A. Starr. 2010. Kinesin-1 and dynein at the nuclear envelope mediate the bidirectional migrations of nuclei. *J. Cell Biol.* 191.

Harada, T., J. Swift, J. Irianto, J.W. Shin, K.R. Spinler, A. Athirasala, R. Diegmiller, P.C.D.P. Dingal, I.L. Ivanovska, and D.E. Discher. 2014. Nuclear lamin stiffness is a barrier to 3D migration, but softness can limit survival. *J. Cell Biol.* 204:669–682. doi:10.1083/jcb.201308029.

Harr, J.C., C.D. Schmid, C. Muñoz-jiménez, R. Romero-bueno, V. Kalck, A. Gonzalez-sandoval, M.H. Hauer, J. Padeken, P. Askjaer, A. Mattout, and S.M. Gasser. 2020. Loss of an H3K9me anchor rescues laminopathy-linked changes in nuclear organization and muscle function in an Emery-Dreifuss muscular dystrophy model. 1–20. doi:10.1101/gad.332213.119.

Hatch, E.M., A.H. Fischer, T.J. Deerinck, and M.W. Hetzer. 2013. Catastrophic Nuclear Envelope Collapse in Cancer Cell Micronuclei. *Cell*. 154:47–60. doi:10.1016/j.cell.2013.06.007.

Ho, J., V.A. Valdez, L. Ma, and D.A. Starr. 2018. Characterizing Dynein' s Role in P-cell Nuclear Migration using an Auxin-Induced Degradation System. 1:2016–2018.

Kwon, M., M.L. Leibowitz, and J.H. Lee. 2020. Small but mighty: the causes and consequences of micronucleus rupture. *Exp. Mol. Med.* 52:1777–1786. doi:10.1038/s12276-020-00529-z.

Link, J., D. Paouneskou, M. Velkova, M. Alsheimer, M. Zetka, V. Jantsch, J. Link, D. Paouneskou, M. Velkova, A. Daryabeigi, S. Labella, C. Barroso, M. Alsheimer, M. Zetka, and V. Jantsch. 2018. Transient and Partial Nuclear Lamina Disruption Promotes Chromosome Movement in Early Meiotic Article Transient and Partial Nuclear Lamina Disruption Promotes Chromosome Movement in Early Meiotic Prophase. 212–225. doi:10.1016/j.devcel.2018.03.018.

Malone, C.J., W.D. Fixsen, H.R. Horvitz, and M. Han. 1999. UNC-84 localizes to the nuclear envelope and is required for nuclear migration and anchoring during C. elegans development. *Development*. 126:3171–3181.

Raab, M., M. Gentili, H. de Belly, H.-R. Thiam, P. Vargas, A.J. Jiminez, F. Lautenschlaeger, R. Voituriez, A.-M. Lennon-Dumenil, N. Manel, and M. Piel. 2016. ESCRT III repairs nuclear envelope ruptures during cell migration to limit DNA damage and cell death. *Science (80-.).* 352:359–362.

Starr, D.A. 2012. Laminopathies: Too Much SUN Is a Bad Thing. *Curr. Biol.* 22:R678–R680. doi:10.1016/j.cub.2012.06.070.

Starr, D.A. 2019. A network of nuclear envelope proteins and cytoskeletal force generators mediates movements of and within nuclei throughout Caenorhabditis elegans development. *Exp. Biol. Med.* 244:1323–1332. doi:10.1177/1535370219871965.

Sulston, J.E., and H.R. Horvitz. 1981. Abnormal cell lineages in mutants of the nematode Caenorhabditis elegans. *Dev. Biol.* 82:41–55. doi:https://doi.org/10.1016/0012-1606(81)90427-9.

Swift, J., I.L. Ivanovska, A. Buxboim, T. Harada, D.P.P.C. Dingal, J. Pinter, J.D. Pajerowski, K.R. Spinler, J.-W. Shin, M. Tewari, F. Rehfeldt, D.W. Speicher, and D.E. Discher. 2013. Nuclear Lamin-A Scales with Tissue Stiffness and Enhances Matrix-Directed Differentiation. *Science (80-.).* 341. doi:10.1126/science.1240104.

Thiam, H.-R., P. Vargas, N. Carpi, C.L. Crespo, M. Raab, E. Terriac, M.C. King, J. Jacobelli, A.S. Alberts, T. Stradal, A.-M. Lennon-Dumenil, and M. Piel. 2016. Perinuclear Arp2/3-driven actin polymerization enables nuclear deformation to facilitate cell migration through complex environments. *Nat. Commun.* 7:10997. doi:10.1038/ncomms10997http://www.nature.com/articles/ncomms10997#supplementary-information.

Ungricht, R., and U. Kutay. 2017. Mechanisms and functions of nuclear envelope remodelling. *Nat. Publ. Gr.* 18. doi:10.1038/nrm.2016.153.

Velez-aguilera, G., S.N. Nkoula, B. Ossareh-nazari, J. Link, D. Paouneskou, L. Van Hove, N. Joly, N. Tavernier, J. Verbavatz, V. Jantsch, L. Pintard, D. Paris, and J. Monod. 2020. PLK-1 promotes the merger of the parental genome into a single nucleus by triggering lamina disassembly. 1–31.

Wiesel, N., A. Mattout, S. Melcer, N. Melamed-Book, H. Herrmann, O. Medalia, U. Aebi, and Y. Gruenbaum. 2007. Laminopathic mutations interfere with the assembly, localization, and

dynamics of nuclear lamins. *Proc. Natl. Acad. Sci. U. S. A.* 105:180–185.